

The copyright of this thesis vests in the author. No quotation from it or information derived from it is to be published without full acknowledgement of the source. The thesis is to be used for private study or non-commercial research purposes only.

Published by the University of Cape Town (UCT) in terms of the non-exclusive license granted to UCT by the author.

**SATELLITE DERIVED SEA SURFACE TEMPERATURE  
AND WIND FIELD VARIABILITY IN THE BENGUELA  
UPWELLING REGION**

**Thesis submitted in fulfillment for the degree Master of Science**

**By**

**Dawid Petrus Mouton**

**Department of Oceanography**

**University of Cape Town**

**South Africa**

**September 2002**

## **ACKNOWLEDGEMENTS**

I would firstly like to thank my supervisor, Prof. Frank Shillington, for his support and advice during the preparation of this thesis.

The Ministry of Fisheries and Marine Resources, IRD (through IDYLE/VIBES) and BENEFIT is thanked for providing me with the necessary funding to pursue my studies. The Ministry is also thanked for allowing me the time of to attend classes/work sessions and to work on this thesis. The staff of the Environmental Section at NatMIRC is thanked for their continuous support and encouragement. A special word of thanks goes to Chris Bartholomae who assisted me in many aspects of the work involved in preparing this thesis.

I would also like to thank my wife and daughter for their support and understanding during the times I had to work on my studies.

## ABSTRACT

Satellite measured sea surface temperature (1982 – 2000) and wind field (1992 – 2000) data were analyzed to study the seasonal, inter-annual and spatial variability of upwelling conditions along the southwestern coast of Africa. The  $1^{\circ} \times 1^{\circ}$  gridded data was provided on a monthly scale for analysis. Analyses included that of SST, southerly winds and wind stress and derived Ekman transport.

Although upwelling was found to be more or less perennial along most of the coast south of  $16^{\circ}\text{S}$ , seasonal variations were observed for both the SST and the upwelling favorable wind conditions. Inter-annual variability is common, and with these datasets it was possible to highlight periods of anomalous conditions. Results indicated that both the seasonal and inter-annual variability between the northern and southern parts of the Benguela system is quite different, with stronger seasonality observed in the southern Benguela. Results highlighted the existence of the known cells of higher potential upwelling at Lüderitz, Cape Frio and around the Cape Peninsula.



# INDEX

	Page
<b>Acknowledgements</b>	I
<b>Abstract</b>	II
<b>1 Introduction, Rationale And Aims</b>	1
1.1 Introduction And Background	1
1.2 Aims And Objectives	4
1.3 Thesis Structure	4
<b>2 Literature Review</b>	6
2.1 Overview Of The Physical Features Of The Benguela Current Region	6
2.1.1 Introduction And Background	6
2.1.2 Topography	8
2.1.3 Macroscale Circulation	10
2.1.4 Boundaries	13
2.1.5 Meteorology And Upwelling Variability	14
2.2 Coastal Upwelling	22
2.3 Satellite Oceanography	27
2.3.1 Background	27
2.3.2 Infrared Radiometry	29
2.3.3 ERS Scatterometers	31
<b>3 Materials And Methods</b>	
3.1 Study Area	33
3.2 Data Used	34
3.2.1 Sea Surface Temperature Data	34

**6 Concluding Remarks**

80

**7 Bibliography**

81

University of Cape Town

3.2.2 Wind Fields	35
3.3 Data Processing And Analysis	36
3.3.1 SST Fields	39
3.3.2 Wind Fields	41
3.3.3 Upwelling Indices	42
<b>4 Results And Discussion</b>	<b>45</b>
4.1 Seasonal Variability	45
4.1.1 Wind Conditions	45
4.1.2 Sea Surface Temperature	55
4.2 Inter-Annual Variability	63
4.2.1 Wind Conditions	63
4.2.2 Sea Surface Temperature	68
4.2.2.1 Sea Surface Temperature Anomalies	68
4.2.2.2 Sea Surface Temperature Upwelling Index	72
<b>5 Summary Of Results</b>	<b>75</b>
5.1 Seasonal Variability	75
5.1.1 Wind Fields	75
5.1.2 Ekman Upwelling Index (EUI)	76
5.1.3 SST Fields	76
5.2 Inter-Annual Variability	78
5.2.1 Ekman Upwelling Index (EUI) and Southerly Wind Stress Anomalies	78
5.2.2 SST Fields	78

# 1 INTRODUCTION, RATIONALE AND AIMS

## 1.1 INTRODUCTION AND BACKGROUND

As with the three other major eastern boundary current regions of the world (Figure 1), the oceanography of the Benguela current region is dominated mainly by coastal upwelling (Shannon 1985; Boyd 1987; Bakun and Nelson 1991; Shannon and Nelson 1996 and Shillington 1998). This upwelling acts to supply large quantities of nutrients to the system, making the Benguela one of the most productive and nutrient-rich upwelling systems in the world. Consequently, it supports a large, productive fishery in the region, both demersal and pelagic.

The coastal upwelling is predominantly driven by the southerly wind stress, with seasonal variations in intensity and distribution in time and space (Shannon 1985; Shannon and Nelson 1996 and Cole and McGlade 1998). To a lesser extent, upwelling is also affected by other factors such as local bathymetry and coastal orientation.

The wind along the coast of southwestern Africa is influenced by the South Atlantic high-pressure system; the seasonal low-pressure field over the subcontinent and southeast moving coastal lows (Shannon 1985; Jury *et al* 1990; Shannon and Nelson 1996). The desert-like conditions of the inland coastal plains act as a thermal barrier, which steers the anti-cyclonic flow of the high-pressure system along the coast, giving rise to the observed southerly wind direction (Nelson and Hutchings 1983). The prevailing climatology/wind regime of the Benguela upwelling system is discussed in

more depth by, amongst others, Shannon (1985), Boyd (1987), Preston-Whyte and Tyson (1988) and Shannon and Nelson (1996) and a synthesis of these and other works will follow later in the thesis.

Environmental variability in the Benguela occurs over a range of spatial and temporal scales. This is largely driven by the atmospheric and oceanographic variability over the region. The effects of such variability have been observed not only in the physical environment, but also in that of the Benguela large marine ecosystem. The frequency and intensity of the observed variability depends to a large extent on the location of the area of interest in the region. For example, seasonal variability in the Northern Benguela appears to have a different signal from that in the Southern Benguela region (Shannon 1985; Shillington 1998). Although much has been written about the variability in the Benguela current region (Boyd 1987; Brundrit 1984; Nelson and Walker 1984; Walker *et al* 1984; Shannon 1985; Shannon *et al* 1986; Boyd 1987; Boyd *et al* 1987; Lutjeharms and Meeuwis 1987; Walker 1987; Brundrit 1995; Cole 1997, Cole and McGlade 1998; Gammelsrød *et al* 1998 and Shillington 1998), more still remain to be understood about this topic.

Given the importance of coastal upwelling in the region, i.e. the pumping of nutrients into the sunlit zone for primary productivity and the dominance of upwelling in coastal oceanographic processes, it is appropriate to investigate the variability of the Benguela in terms of its upwelling features and the upwelling favorable conditions at the coast. Coastal upwelling is caused by the effect of the equatorward, alongshore component of the wind stress on the sea surface, the proximity of the coastal boundary and the Coriolis force. Through the process of upwelling, cool nutrient rich

water ascends to the surface, causing a reduction in the sea surface temperatures at the coast where the upwelling occurs.

The upwelling variability in the Benguela region was therefore studied in terms of the variability of the coastal sea surface temperatures (SST's) and the upwelling favorable wind fields. Although upwelling is not only affected by the alongshore wind and not only manifested in the reduction of SST's, these are by far the more important and easiest to measure. The author is well aware of the effects of seasonal variations on solar heating on local SST's and will thus refer to it in the text where appropriate. Wind parameters included here for analysis are the meridional components of the wind speed and wind stress.

The study area included much of the South-east Atlantic (Figure 6). This was mainly to provide a greater spatial overview and to include boundary regions interacting with the known Benguela current region. Analysis was performed in such a way to enable the author to give an overview of the conditions under study over the entire study area. However, greater emphasis was placed on the coastal region where coastal upwelling occurs.

The temporal scales of interest here is that of seasonal and inter-annual. An overview is given of the mean seasonal patterns of each parameter. Further analysis highlighted the inter-annual variability over the region and enabled the identification of years during which significantly anomalous conditions occurred.

Nineteen years (January 1982 to December 2000) of one degree gridded Reynolds and Smith (1994) monthly sea surface temperature (SST) fields, extracted from the NOAA NCEP re-analysis web site were analyzed for the identification and description of the mean SST conditions and the variability of the SST condition at the different scales mentioned earlier. The SST fields are continuously updated on the mentioned website. Analyses on the mean equatorward wind fields were done using the one-degree gridded scatterometer measurements from the ERS 1 and ERS 2 scatterometers. The study period was between January 1992 and December 2000, constituting a nine-year dataset of monthly data.

## **1.2 AIMS AND OBJECTIVES**

The main aims of this study are:

1. To explore satellite derived sea surface temperature (SST) and wind field data as indices for the large-scale temporal and spatial variability of upwelling in the Benguela current region.
2. To determine the seasonal, inter-annual and latitudinal variability in the upwelling conditions along the coast.
3. To identify anomalies in these conditions over the study period.

## **1.3 THESIS STRUCTURE**

Following the initial introduction in Chapter 1, Chapter 2 provides an overview on the Benguela upwelling region, its physical features, climatology and associated variability. It further attempts to give a brief overview on the theoretical aspects of

upwelling mechanisms and some background on satellite remote sensing in oceanography, and the sensors and techniques used in collecting the data used in this study. Chapter 3 then follows with a description of the data and the methods used in preparing and analyzing the data. The results of the study are discussed in Chapter 4 with a summary of these results in Chapter 5. Some concluding remarks follow in Chapter 6, wrapping up this thesis.

University of Cape Town



## 2 LITERATURE REVIEW

### 2.1 OVERVIEW OF THE PHYSICAL FEATURES OF THE BENGUELA CURRENT REGION

#### 2.1.1 INTRODUCTION AND BACKGROUND

The physical features of the Benguela region have been reviewed thoroughly by a number of authors (e.g. Nelson and Hutchings 1983; Boyd 1987; Shannon and Nelson 1996; Shillington 1998 and Cole 1997) and the reader is referred to the numerous publications cited by them. The section that follows is an attempted synthesis of these and other works. This should serve mainly as background to this study and to put further analyses in the correct context.

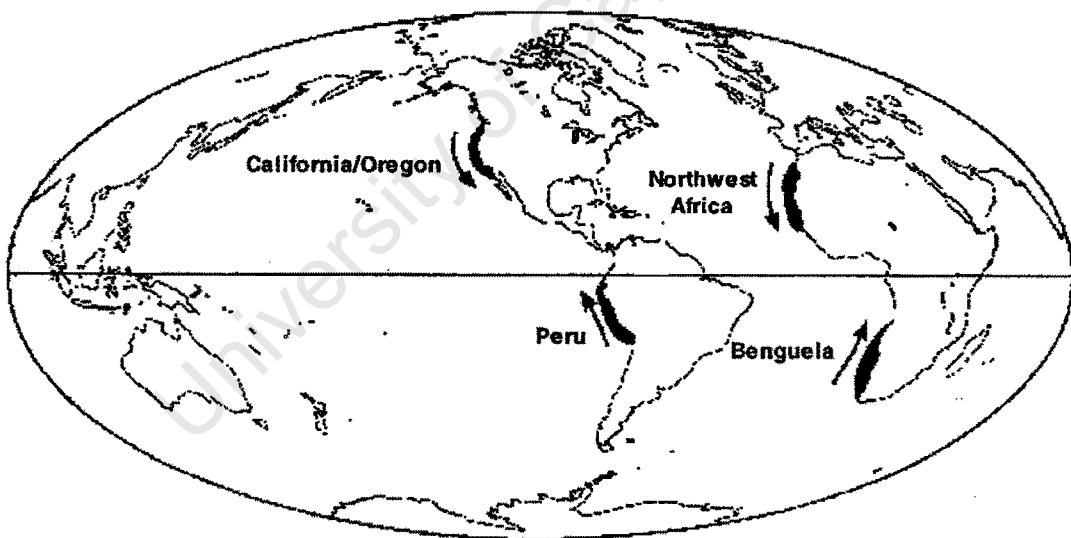


**Figure 1** Major Eastern Boundary Current Regions of the World (From Cole, 1997).

The Benguela is one of the four major eastern boundary current regions of the world (Figure 1). The oceanography is, as with the other three systems, dominated by wind-driven coastal upwelling processes (Shannon 1985). The Benguela system is unique

amongst the four major eastern boundary current regions, in that it is bounded on both equator-ward and pole-ward ends by warm water masses.

According to Hart and Currie (1960) (from Shannon 1985), the Benguela can be described as a "... region of cool upwelled coastal water along the South-west coast of Africa". These waters, which are characterized by a marked negative surface temperature anomaly, are mainly found between 15 °S and 34 °S within 185 km of the coast (Shannon 1985). Shannon and Nelson (1996), in their review paper, took the Benguela to be that "part of the South-east Atlantic lying between about 14 °S and 37 °S, with a western boundary at the 0 ° meridian". Definitions based on the northward flow of the currents have been introduced by other authors (see Shannon 1985). Other, more encompassing definitions exist, for example that proposed by Bang (1971). It is realized that the northward flow over the inner shelf (Shannon 1985; Boyd 1987 and Shannon and Nelson 1996) is a distinct characteristic of the Benguela and that it is alternated with offshore divergence. Although coastal upwelling is limited to that area close to the coast, its influence on the surrounding system can be observed for hundreds of kilometers offshore.

For the purpose of this thesis, the Benguela is considered to be that area lying roughly between 14 °S and 34 °S, with a western boundary at the 0 ° meridian. In the light of the above discussion and for the purpose of easier delineation and analysis, the western extent of that area most strongly affected by the coastal upwelling processes, is taken to be about 185 km from the coast.

### 2.1.2 TOPOGRAPHY

The eastern boundary of the Benguela system is formed by the western coast of the sub-continent (Figure 2). This is characterized by a narrow coastal plain, rising to the main continental escarpment situated between 50 km and 200 km inland. Most of the coastal region is arid with the Namib Desert extending between 14 °S and 31 °S. It is widest in the central region (Shannon 1985 and Boyd 1987). The coastline north of 32 °S is regular with the only significant embayments at Walvis Bay and Lüderitz. South of 32 °S, the coastline is much more irregular with several capes (*e.g.* Cape Columbine, Cape Peninsula, and Cape Hangklip) and embayments (*e.g.* St. Helena Bay, Saldanha Bay, Table Bay, and False Bay). The topography along the coast plays an important role in the local wind forcing, particularly so at the upwelling centers in the system (Shannon 1985).

The **bathymetry** of the continental margin is variable (Figure 2) (Shannon 1985; Boyd 1987 and Shannon and Nelson 1996). The main bathymetric features can be summarized as follows. Narrow parts of the continental shelf are found off Southern Angola (20 km), south of Lüderitz (75 km) and off the Cape Peninsula (40 km). At the Kunene margin, the shelf is about 45 km wide, 200m deep with a relatively steep continental slope. The Walvis shelf, between Cape Frio (18 °S) and Chamais Bay (28 °S), is typically 140 km wide, on average relatively deep, with shelf breaks at about 350 m. Double shelf breaks are common. Around Walvis Bay (23 °S) an inner shelf break can be found at a depth of about 140 m with an outer shelf break at approximately 400 m depth. The Orange River shelf, situated between Chamais Bay and Hondeklip Bay, is at its widest about 180 km wide. Between 32 °S and 35 °S, the

shelf width is variable. A double shelf break, at between 200 and 380 m and at 500 m, is found between 31 °S and 33 °S. It merges south of 33 °S to form a single, deep shelf break at about 500 m. At the southernmost section of the system is the Agulhas Bank, which is relatively wide and shallow.

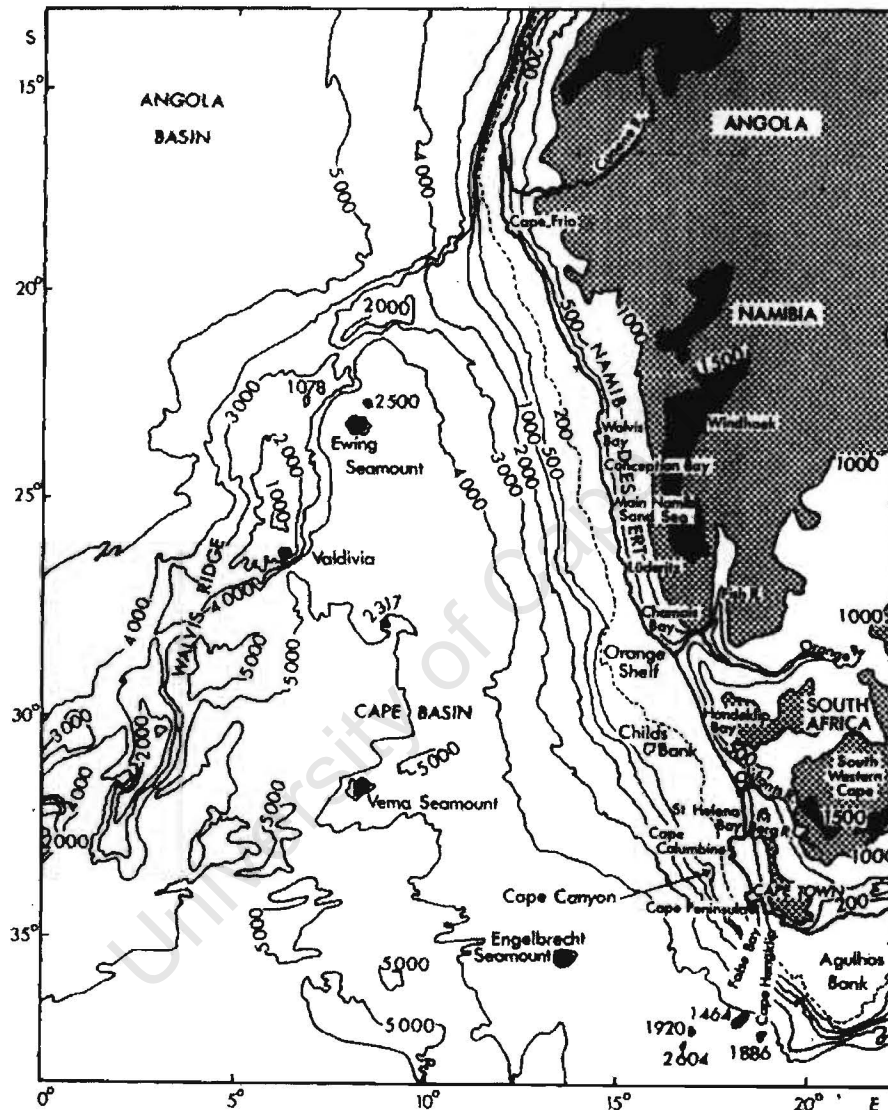


**Figure 2** The Bathymetry of the South East Atlantic Ocean and Main Orographical Features of Southwestern Africa (From Shannon, 1985).

The South East Atlantic abyssal plain, comprised of the Angola and Cape Basins, is separated by the Walvis ridge (Figure 2). This ridge, which runs from the coast at

about 20 °S in a southwesterly direction towards the Mid-Atlantic Ridge, forms a barrier to cross-flow, both northward and southward, below depths of 3000 m (Shannon 1985 and Shannon and Nelson 1996).

### **2.1.3 MACROSCALE CIRCULATION**

Figures 3a and 3b show the probable pathways of waters at the surface and at depths between 200 m and 300 m respectively. This was taken from the review of Shannon (1985) who synthesized and combined the results from a number of articles from various authors.

#### **2.1.3.1 Surface Circulation**

An overview of the surface circulation in the SE Atlantic is provided by figure 3a. A well-defined current in a band 200 km - 300 km wide flows in a north northwesterly direction next to the coast at 34 °S. Northwards, it progressively moves offshore. North of 20 °S, the currents tend to move more westwards. Between 35 °S and 20 °S, there appear to be a divergence of currents with westward flow to the west of this divergence line. Again a significant westward flow at the surface can be observed between 23 °S and 15 °S. This westward flow seems to be separated from the South Equatorial Countercurrent further north by a large cyclonic gyre.

Nelson and Hutchings (1983) suggest that these currents are influenced strongly by topography (will accelerate over steep topography and meander over the planes; the influence of the Walvis ridge) and winds (in the absence of strong current gradients away from the coast).

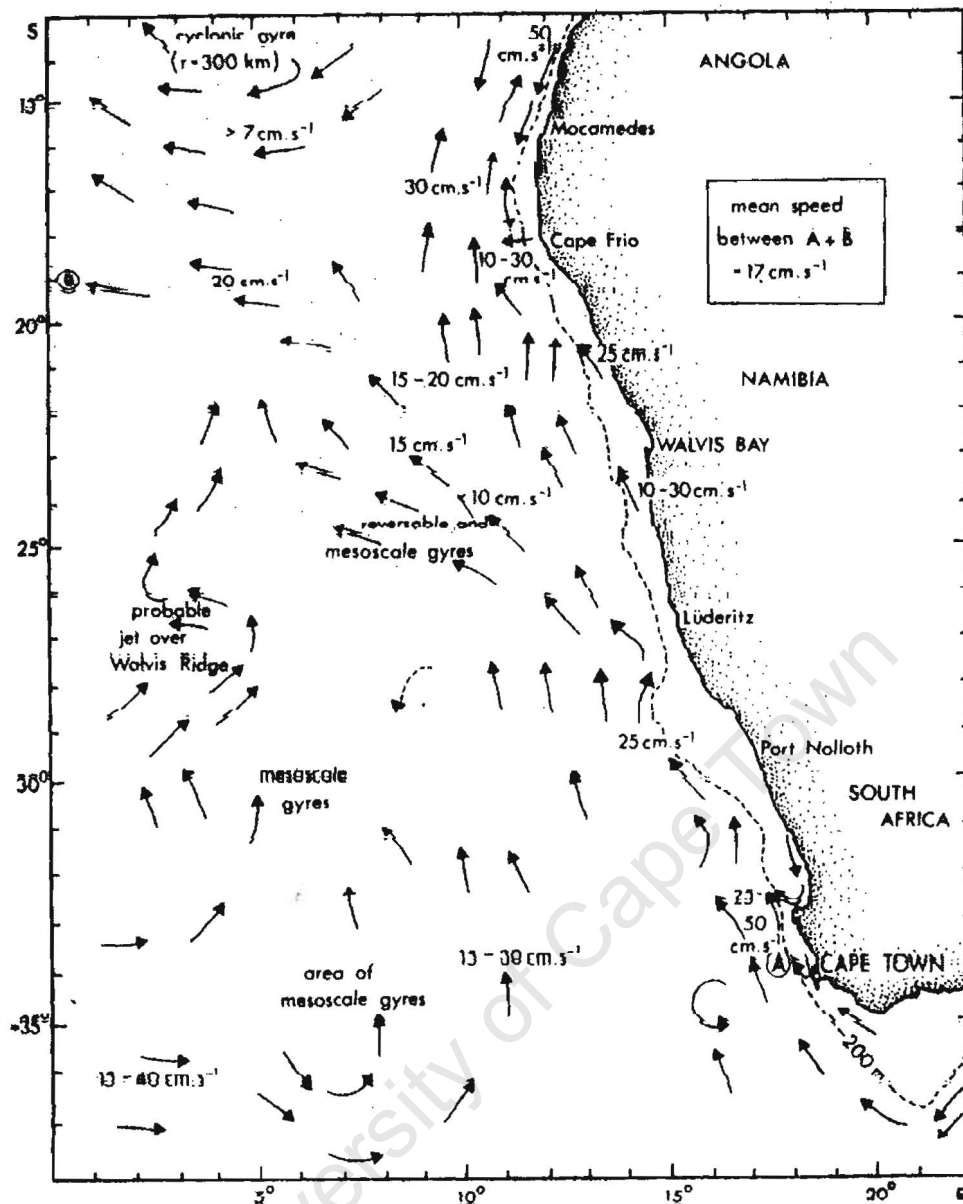


**Figure 3a** Conceptual View of the Surface Currents in the South East Atlantic (From Shannon, 1985).

### 2.1.3.2 Circulation between 200 m and 300 m depth

Figure 3b is a schematic representation of the circulation between 200 m and 300 m depth.

South of 20 °S, the flow is not much different from that of the surface currents. The “current band” adjacent to the coast however is absent. North of this latitude however, differences in the flow patterns become evident. West of 10 °S and south of

the anti-cyclonic gyre (13 °S: 4 °E), a predominantly westward flow can be observed (Moroshkin *et al*, 1970). West of the shelf break, a poleward undercurrent parallel to the coast exists as far south as Lüderitz (Hart and Currie 1960 and Nelson and Hutchings 1983).

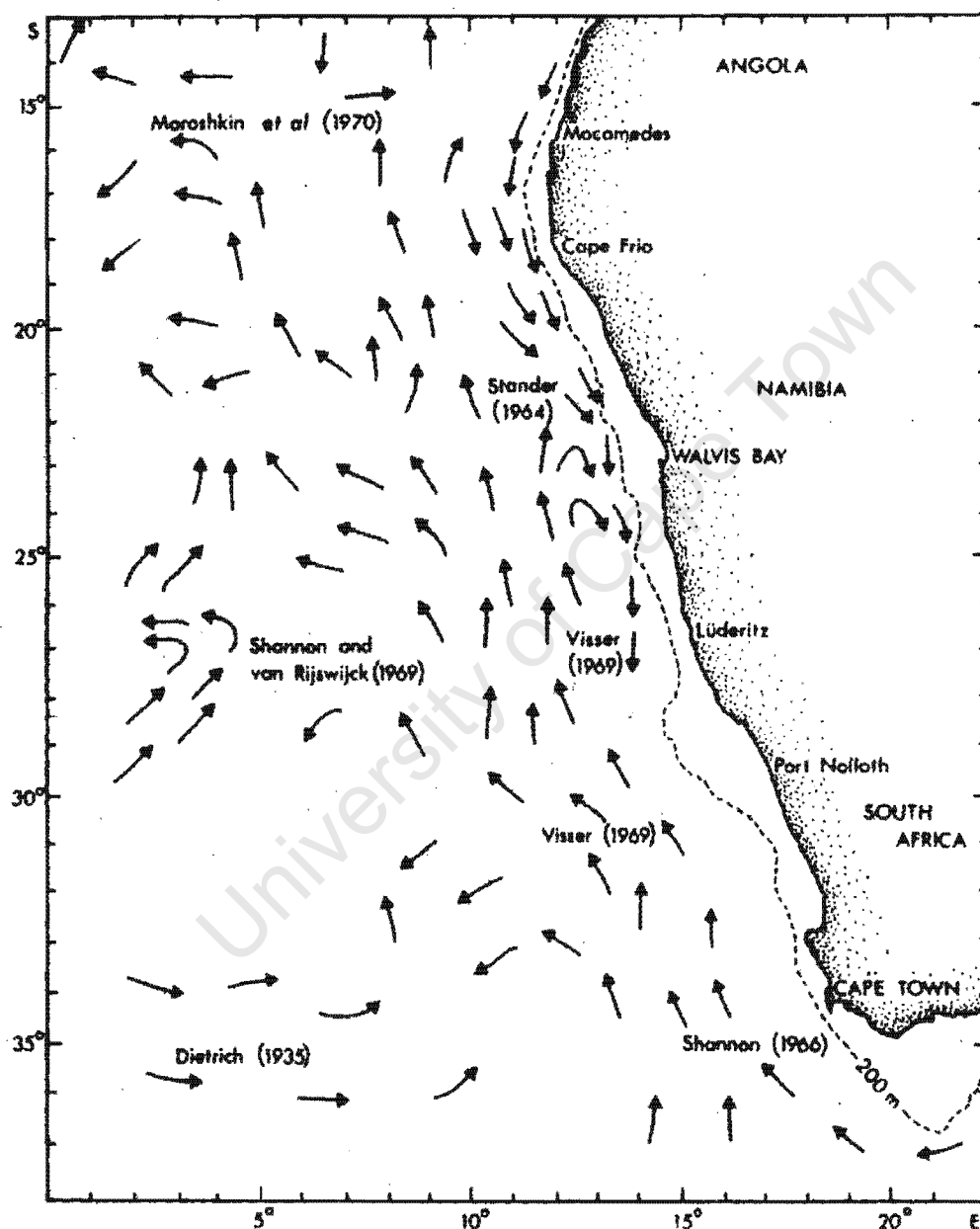


**Figure 3b** Probable Movement of the Central Waters between 200 m and 300 m  
(From Shannon, 1985).

In addition to figures 3a and 3b, the reader is also referred to the articles mentioned in the text for more complete discussions.

#### **2.1.4 BOUNDARIES**

According to Shillington (1998), the nature of the Benguela upwelling system is to a large extent affected through its boundaries. In their review articles, Shannon (1985), Shannon and Nelson (1996) and Shillington (1998), discussed in reasonable detail those boundaries that surround the system. Whereas some authors may focus mainly on those boundaries to the southern, northern and western ends of the system, these authors went further and included in their delineation of the boundaries, that of the upper ocean surface and a bottom boundary.

Shillington (1998) considers the upper ocean surface boundary as where the cyclonic wind stress curl introduces potential vorticity, causing uplifting in the thermocline near the coast. Here, through atmospheric controls, the cyclonic wind stress curl patterns supply the Ekman pumping that enhances upwelling.

As a bottom boundary, he suggests the poleward undercurrent, which is the poleward flow of oxygen-depleted water over the bottom on the shelf (Nelson 1989).

In the north, the Benguela current is bounded by the warm, southward flowing Angola current. The Angola and Benguela currents are separated by a front that is normally found around 16 °S, known as the Angola-Benguela Frontal Zone (Shannon *et al* 1987; Meeuwis and Lutjeharms 1990 and Shillington 1998). Although variable in position, spatial extent and intensity of the temperature gradient, the front is persistent throughout the year and in the upper 50 m between 15 °S and 17 °S (Shannon *et al* 1986 and Shannon *et al* 1987). It normally moves southward during summer (usually



reaches its maximum southward position during March). During years of strong warm anomalies (Benguela Niño) the front is poorly manifested and at the peak of such an event, may even almost disappear (Shannon *et al* 1986 and Gammelsrød *et al* 1998).

At the southern extremity of the system, it is bounded by the warm, Agulhas current. The main contribution that the Agulhas current makes, is by providing warm, more saline waters to the system through eddy type features or Agulhas rings that break off from the main system and get entrained into and transported north and northwestward by the Benguela current (Shillington 1998).

On the open ocean end of the system, like in other upwelling systems, outer frontal regions provide a boundary between the cool upwelled water and the warmer oceanic waters (Shillington *et al* 1990 and Shillington 1998). This is easily spotted when studying infrared satellite images of sea surface temperature (e.g. in van Foreest *et al* 1984; Meeuwis and Lutjeharms 1990 and Shillington *et al* 1990). Van Foreest *et al* (1984), Lutjeharms and Stockton (1987) and Shillington *et al* (1990) amongst others, have documented on these in the past.

#### **2.1.5 METEOROLOGY AND UPWELLING VARIABILITY**

In general the prevailing wind system over the Benguela is influenced by the South Atlantic High Pressure System (anticyclones), the pressure field over the adjacent subcontinent and eastward moving cyclones (Shannon 1985; Preston-Whyte and Tyson 1988 and Shannon and Nelson 1996).

Although the South Atlantic High Pressure System is maintained throughout the year, seasonal shifts are experienced (Shannon 1985, Boyd 1987 and Preston-Whyte and Tyson 1988). Seasonal differences in pressure ranges between 3 and 4 mb (Preston-Whyte and Tyson 1988). There is an approximate latitudinal shift of  $6^{\circ}$  northward in winter (May), when the high-pressure system is roughly centered on  $25^{\circ}\text{S}$  (Shannon 1985; Preston-Whyte and Tyson 1988). During summer it is centered on  $31^{\circ}\text{S}$ . Zonal shifts also occur and during summer the approximate position of the core of the high-pressure cell is around  $4^{\circ}\text{E}$  and in winter around  $13^{\circ}\text{E}$ . Because of the radical change of the pressure field over the subcontinent from a well developed low in summer to a weak high in winter, the pressure gradient also show significant seasonal variability. Resultant curved anticyclonic flow is directed north to northwest as a result of the coastline, which, due to its desert like conditions, acts as a thermal barrier to cross flow (Nelson and Hutchings 1983, Preston-Whyte and Tyson 1988). Winds are predominantly southerly to southwesterly, and thus upwelling favorable. The cyclic weather pattern over the Benguela during summer is illustrated in Figure 4. It is obvious that marked seasonal variations occur in both the position and strength of the South Atlantic High Pressure system. Consequently one would expect to detect a similar degree of seasonality in the wind fields and upwelling conditions along the coast. However, although a clear seasonal cycle can be observed in the wind field over the Southern Benguela, the same is not entirely true for the Northern Benguela. More on this will follow later in this section. On the other hand, seasonality in the SST fields is more common as it is not only influenced by upwelling but also by changes in the amounts, frequency and persistence of solar heating.

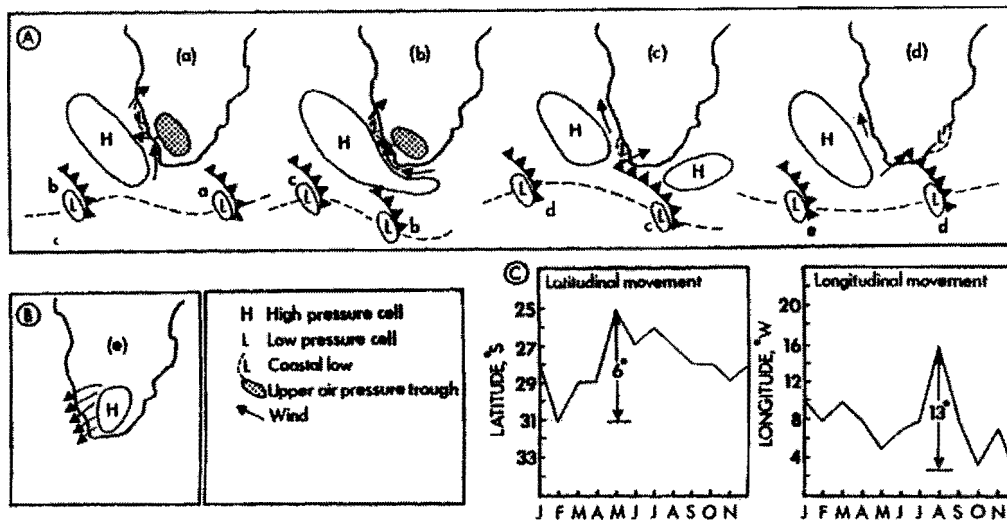


**Figure 4** The Cyclic Weather Pattern of Southern Africa (From Shannon and Nelson, 1996).

Upwelling systems in general show intense variability at mesoscales with seasonal variation quite obvious at mid- and high latitudes (Abbott and Barksdale 1995). Variability in the Benguela, as in other coastal upwelling systems, occurs at a variety of temporal and spatial scales (Abbott and Barksdale 1995 and Shillington 1998). Temporal scales include diurnal, synoptic, event, seasonal, inter-annual and episodic event scales. Additionally, latitudinal as well as longitudinal variations are observed and seem to coincide with the seasonal variations in the upwelling favorable winds and solar heating. The variability of wind events is dominated mainly by the atmospheric synoptic scale of 3 – 10 days, and sometimes extends to a few weeks (Shillington, 1998). Variations in SST's are brought about by both seasonal changes in solar heating and upwelling activity (at the coast). In the sections to follow, an

attempt is made to highlight those scales of variability that is of some importance to the oceanography off the coast of southwestern Africa. Hart and Currie (1960), from their analysis of coastal wind speeds during summer and winter found that during winter the effect of the northward shift in the pressure system is much more pronounced in the south when a higher frequency of westerly winds are experienced. Here the wind induced upwelling is much more seasonal with a maximum during spring and summer (September to March) (Andrews and Hutchings 1980). The seasonal variability north of 31 °S appears to be less pronounced (Shannon and Nelson 1996). Although upwelling here is perennial along most of the coast, a summer maximum and autumn minimum south of 25 ° S and a late winter-spring maximum north of 25 ° S can be observed in local winds. Slight maxima in upwelling favorable winds are experienced during April-May and October over central Namibia. Alongshore winds near Cape Frio in the north are strongest during autumn and spring (Boyd 1987). These differences in the seasonal patterns of the upwelling favorable conditions along the coast effectively divide the system into a northern and southern part.

Wind relaxation or reversals of about a week during the upwelling season serve to effectively modulate upwelling in the southern Benguela (Shannon and Nelson 1996). This usually is associated with approaching cyclonic systems south of the sub-continent. Related to these are cells of low pressure systems developing around Lüderitz and moving southward and around the subcontinent as coastal trapped waves (Reason and Jury 1990). This is best seen during summer as the modulation provided by the South Atlantic high pressure system weakens. The cyclonic rotation of air about these cells has a suppressing influence on local upwelling.

Diurnal variations (land-sea breezes) in the winds are common along most of the coast north of Cape Columbine (Hart and Currie 1960). Shannon (1985) reasons that this diurnal pulsing of winds and the seasonal variations exhibited must be important for the coastal upwelling system. Boyd (1987) from his analysis of coastal and shipboard measurements of the local winds along the Namibian coast gave a good overview of the diurnal pulsing of the winds over the central Namibian coast. He found that these are significant with increased onshore flow at the central Namibian coast towards the afternoon.

A noticeable feature of the Benguela is the occurrence of “berg” winds, locally known as “east winds”, during autumn and winter. These winds blow off the western escarpment when high pressure cells form over the subcontinent. This dry, adiabatically heated air blows over the coastal areas and the adjacent ocean, carrying large quantities of dust and sand out to the sea. Nelson and Hutchings (1983) have suggested that these winds might suppress upwelling in the southern parts of the Benguela. Boyd (cited by Shannon 1985) on the other hand has suggested that these winds can in fact produce localized upwelling, but its effect will be limited to only about 10 km off the coast.

The comparative climatology of the Benguela and other boundary current regions has been discussed by Parish *et al* (1983) described. From their computed Ekman transported they concluded that in the Benguela region:

- The Lüderitz area appears to be the principle potential upwelling center, with a secondary region at Cape Frio.

- North of 28 °S, a pronounced zone of offshore divergence exists, supporting the idea of increased anticyclonic rotation in the wind field with increasing distance offshore.
- The wind stress maximum is to be found in a band away from the coast, evident particularly during winter.
- Near-shore Ekman transport north of Lüderitz does not change very much between winter and summer. However, south of Lüderitz the difference becomes significant.

Bakun and Nelson (1991) extended the work of Parish *et al* (1983) by studying the seasonal variability of the wind stress and wind stress curl in subtropical eastern boundary current regions. Their work yielded similar results. These authors reported on the coastal wedge-shaped area of strongest cyclonic wind stress curl just south of 25 °S (near Lüderitz). This 200 km wide wedge reaches its most southern extent (around the Cape Peninsula) from late spring to early autumn, with its most limited southward extent in winter. Other areas of significant cyclonic wind stress curl are north of Cape Frio (near 15 °S) and in the south of the subcontinent, both areas forming the approximate latitudinal boundaries of the Benguela system. Results from both the above studies are in good agreement for example with what Boyd (1987) found along the Namibian coast.

The wind field over southern Benguela system has been studied relatively well (*e.g.*, Kamstra 1985; Hunter 1987; Jury 1988; Hutchings and Taunton-Clark 1990 and Johnson and Nelson 1999). However, fewer studies exist on that over the northern Benguela (see Nelson and Hutchings 1983; Shannon 1985 and Shannon and Nelson

1996). Boyd (1987), from the analyses of anemometer and ships data, made a great contribution to the understanding of the prevailing wind conditions over the Namibian coastal and shelf region.

On the northern end of the system, the position of the Angola-Benguela Frontal Zone (ABFZ) is known to shift seasonally (Shannon *et al* 1986; Shannon *et al* 1987; Boyd *et al* 1987 and Shillington 1998). Meeuwis and Lutjeharms (1990) documented its northern boundary to be around 14 °S and the southern boundary near 16 °S. This of course changes seasonally and the front is known to reach its most southerly extent during late summer – early autumn (Meeuwis and Lutjeharms 1990). A similar seasonal shift appears not to happen at the southern extremity of the system (Shillington 1998).

Inter-annual variations in the synoptic scale wind fields do occur over the larger Benguela region (Shannon and Nelson 1996 and Shillington 1998). Mean seasonal conditions can vary from year to year. This is regarded as normal. However, occasionally these variations are stronger than ‘usual’ resulting in either abnormally warm or cold years or seasons. The most significant of these variations appear to be related to the El Niño Southern Oscillation (ENSO). During El Niño (low phase) alongshore winds in the extreme south of the system weaken (Shannon and Nelson 1996). During the high phase (La Niña) these winds tend to strengthen. The ENSO is further known to cause significant variations in precipitation over the South-East Atlantic (Gamelsrød *et al* 1998). Over the years it has been established that the Pacific El Niño has a counterpart in the South-East Atlantic, referred to as Benguela Niño’s (Shannon *et al* 1986). These events are less frequent and less intense than

their Pacific counterpart, and are characterized by the intrusion of warm, saline water from the north and northwest (Shannon *et al* 1986, Boyd *et al* 1987 and Gamelsrød *et al* 1998). Their periodicity is variable, but Shannon *et al* (1986) suggest that it occurs at least once in ten years. Due to its characteristic approach from the north, Benguela Niño's have the strongest effects in the northern Benguela system with little effects on the southern part of the system. On the other hand, the southern Benguela appears to be affected more regularly by ENSO events with the northern Benguela showing some out of phase characteristics with regards to ENSO events (Shannon *et al* 1986). Significant Benguela Niño's that has been well documented appeared to have occurred in 1934, 1949, 1963, 1984 and 1995 with less well documented events around 1910, in the 1920's and in the early 1970's (Gamelsrød *et al* 1998). What is even less documented is the occurrence of so-called cool events in between major warm events. The most recent one was recorded in 1997.



## 2.2 COASTAL UPWELLING

Coastal upwelling is the process by which sub-surface water moves vertically over the shelf slope to the surface (Cole 1997) and is transported horizontally away from the coast through surface flow (Barber and Smith 1981). Through this process, large quantities of nutrients are supplied to the euphotic zone of the water column, stimulating/facilitating high levels of phytoplankton production (Mann and Lazier 1991; Cole 1997). Optimal nutrient and light conditions are maintained for sufficiently long periods in the stabilized horizontal divergent flow of the surface layer, maintaining significant levels of phytoplankton production and growth (Barber and Smith 1981). Areas of significant upwelling activity are therefore characterized by high levels of primary productivity and, although limited in species diversity, can support relatively large populations of fish, seabirds and marine mammals (Mann and Lazier 1991; Cole 1997).

The Benguela region is one of four major upwelling regions situated along the eastern boundaries of the Atlantic and Pacific oceans (Figure 1) (Bakun and Nelson 1991; Hill *et al* 1998). Coastal upwelling in these eastern boundary current regions is driven by the equatorward winds blowing along the coast (Figure 5) (Barber and Smith 1981; Mann and Lazier 1991; Smith 1995 and Hill *et al* 1998). The resulting frictional stress over the sea surface induces an alongshore surface flow. Due to the Coriolis effect, this surface flow becomes progressively deflected offshore, resulting in the offshore transport of near-coastal water (Mann and Lazier 1991 and Smith 1995). In order to compensate for the water being moved offshore, deeper water over the continental shelf is brought to the surface.

When the alongshore wind blows persistently for a sufficient amount of time, the net movement of the surface water is at right angles to the direction of the wind (Barber and Smith 1981; Mann and Lazier 1991 and Smith 1995). This is termed Ekman transport. V. W. Ekman, in 1905, laid the theoretical basis for this concept by finding a mechanism by which a balance between the forces of the wind drag, water movement and the Coriolis force could be attained (Pond and Pickard 1983; Mann and Lazier 1991). The relationship between these is summarized (illustrated) in Figure 5. Note that it also includes the existence of a thermal front between the cooler, upwelled water and the warmer, oceanic water. This thermal front is never fixed and may sometimes even be difficult to define as a result of the fact that upwelling activity can be influenced by a number of factors.

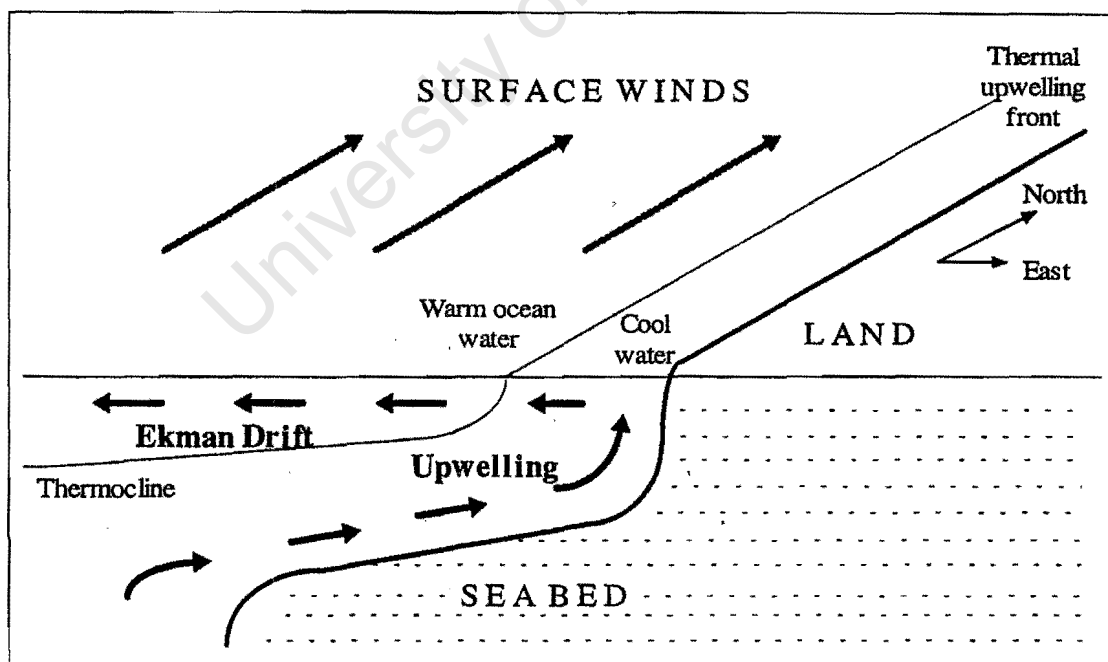


**Figure 5** Schematic Depiction of Eastern Boundary Coastal Upwelling in the Southern Hemisphere (From Cole, 1997).

The layer of water affected by the wind forcing is referred to as the Ekman layer. The net flow in the Ekman layer is at  $90^\circ$  to the left of the wind direction in the southern hemisphere. This net flow is termed the Ekman drift. Ekman transport refers to the mass/volume of water moving offshore per unit time and per unit length of coastline due to Ekman drift (Pond and Pickard 1983; Mann and Lazier 1991). Ekman transport ( $M_E$ ) is estimated from the upwelling inducing wind stress ( $\tau$ ) and the Coriolis parameter ( $f$ ) and is given by  $M_E = -\tau/f$  (Pond and Pickard 1983). Ekman transport has been used on several occasions as an index of upwelling (e.g. Nykjær and Van Camp 1994 and Johnson and Nelson 1999). Hill *et al* (1998) referred to this index of upwelling as “a long-term average at a given location of monthly mean Ekman transports derived from observed winds and expressed in units of  $\text{m}^3\text{s}^{-1}$  per 100m of coastline”. The underlying assumptions are that upwelling is mainly a function of the alongshore wind stress and that the volume of upwelled water is proportional to that volume of water displaced offshore due to Ekman drift.

Upwelling is not a constant process along a straight coast under the influence of constant equatorward, alongshore winds. It is a variable process (Mann and Lazier 1991 and Abbott and Barksdale 1995) during which a number of factors can produce variations in the occurrence, intensity and spatial extent of upwelling. These factors can include changes in the strength of upwelling favorable winds, changes in bottom bathymetry, instabilities in local currents, changes in coastline orientation, and the topography of adjacent coastal regions (Mann and Lazier 1991; Shannon 1985; Cole 1997). Variations on seasonal and shorter time scales are common (Shannon 1985). Shannon (1985) showed that storms and diurnal variations in the thermal conditions

over the ocean could also variations in upwelling activity off the coast of southwestern Africa.

Upwelling systems are known to show variability on a wide range of spatial and temporal scales (Abbott and Barksdale 1995 and Shillington 1998). It is mainly characterized by intense mesoscale variability with obvious seasonality. In general, both small-scale events and large-scale forcing affects upwelling and upwelling variability (Abbott and Barksdale 1995). Seasonal variability is strongly related to the seasonal variations in the high-pressure systems that drive the upwelling favorable winds. The resulting latitudinal shifts in the upwelling favorable winds introduce the seasonal signatures of the upwelling centers along the coast. Longitudinal variations in the wind stress and wind-stress curl are also present as a result of the variation in the pressure system (Abbott and Barksdale 1995). The resultant increase in equatorward wind stress offshore leads to strong gradients in the Ekman transport and hence strong upwelling at the coast.

Inter-annual variability changes the seasonal patterns from year to year and is common in the Benguela and other eastern boundary current regions (Shannon *et al* 1986). The most significant of these are the El Niño Southern Oscillation (ENSO) events, which affect both the strength and position of the upwelling favorable winds. Weakening of or the reversals in the direction of the equatorial trade winds introduce anomalously warm conditions over the ocean. In the Benguela, events related to or showing a resemblance to the ENSO events, are termed Benguela Niño's (Shannon *et al* 1986). The periodicity of such events ranges between 3 and 10 years and is associated with a deepening in the thermocline, warm water intrusions and a reduction

in upwelling activity. Boyd *et al* (1987) and Gammelsrød *et al* 1998, amongst others, have shown that the effects of such events on the biota of the effected region can be devastating. Thus, remotely forced variability such as warm water intrusions (Shannon 1985; Shannon *et al* 1986 and Gammelsrød *et al* 1998), coastal-trapped waves and changes on the depth of the mixed layer, are all factors affecting the upwelling variability of the Benguela and other eastern boundary current regions.

## **2.3 SATELLITE OCEANOGRAPHY**

### **2.3.1 BACKGROUND**

Lillesand and Kiefer (1994) defines remote sensing as “the science and art of obtaining information about an object, area, or phenomenon through the analysis of data acquired by a device that is not in contact with the object, area, or phenomenon under investigation”. Maul (1985) defines remote sensing in oceanography as “the acquisition of information about the sea through the use of sensing devices remote from the feature of interest”.

Remote sensing from space first took off with the use of aerial photography. In fact, around 1882 some pioneers in this field first used cameras mounted to kites to take aerial photographs of the ground (Maul 1985). The use of aerial photography continued to develop and received a major boost during World War I. Remote sensing continued to be driven mainly by military needs.

Satellite remote sensing really only took off with the launch of the Russian satellite, Sputnik in 1957. During the 1970's it started maturing as an operational system for repetitive collection of information about the earth, for purposes other than military. Since then, remote sensing has become a useful tool for collecting data used in a wide array of disciplines (Hardman-Mountford 2000). These ranging from meteorology, land cover mapping and assessment to epidemiology (Lillesand and Kiefer 1994 and Hardman-Mountford 2000).

The first quantitative application of remote sensing in oceanography was made during World War II when attempts were made to do aerial hydrographic surveys (Maul 1985). Research applications already took off in 1952 when H. L. Cameron used aerial photographs of surface drifters to quantify surface circulation in harbors (Maul 1985). Applications continued to develop and later included the fields of marine geology and sea surface climatology (in 1953) (Maul 1985). Breaker and Gilland in 1981 (from Abbott and Barksdale 1995) illustrated one of the earliest discoveries made from infrared satellite observations when they documented on cold filaments along the west coast of North America. Today, satellite remote sensing is used as a tool in a wide range of marine applications and is now commonly used to study the dynamics of upwelling systems.

Initially, applications of satellite remote sensing in oceanography mainly involved the measurement of SST from infrared radiometry (AVHRR, ATSR IRR). However, its applications continued and still continues to expand and today include ocean color and sea ice from visible radiometry (CZCS, SeaWiFS), dynamic heights from radar altimetry (GEOSAT, ERS-1/2 RA, TOPEX/Poseidon), brightness emissivity derived sea ice and global SST from passive microwave sensors (SMMR, SSM/I, ATSR MWS), sea surface roughness and winds from synthetic aperture radar (SAR, e.g. ERS-1/2 SAR, SeaSAT SAR) and sea state from scatterometers (ERS-1/2, NSCAT and QuickScat scatterometers) (Hardman-Mountford 2000).

There have always been concerns amongst users and scientists with regards to the ability of satellite sensors to observe and resolve important scales of variability and, to characterize the patterns of events rather than just resolving specific events. Today,

these concerns are still valid and, although the situation has improved much, problems still exist when trying to use remotely sensed data to describe the characteristic patterns of variability in upwelling systems. Despite this, the successful applications of satellite data in coastal studies have grown significantly over the last couple of decades. In upwelling system, applications include, amongst others, the identification and description of both mesoscale features such as fronts, jets and filaments, and smaller-scale processes (e.g. frontal instabilities). Works by Breaker and Gilland in 1981 (from Abbot and Barksdale 1995) and Van Camp *et al* (1991) are only a few examples of this. Numerous others can be cited. In the Benguela system, satellite remote sensing data have played an important role over the last two or so decades in identifying and describing events and features that are common in the region. Applications were mainly geared towards studies on filaments (e.g. Lutjeharms and Stockton 1987; Shillington *et al* 1990 and Lutjeharms *et al* 1991); seasonal and inter-annual SST variability (e.g. Lutjeharms and Meeuwis 1987; Walker 1987 and Cole and McGlade 1998) and the investigation of anomalously warm conditions (e.g. Gammelsrød *et al* 1998) amongst others.

The following two sections contains brief descriptions of the sensors involved in the collection of the data described in this thesis, i.e. SST and wind fields. More comprehensive discussions are contained in the literature cited in the text.

### **2.3.2 INFRARED RADIOMETRY**

NOAA's Advanced Very High Resolution Radiometer (AVHRR) is a broad-band, four or five channel scanner, sensing in the visible, near-infrared, and thermal infrared



portions of the electromagnetic spectrum (Kidwell 1991). This sensor is carried on NOAA's Polar Orbiting Environmental Satellites (POES), which started in 1978 with TIROS-N. The sensors on board have a measuring accuracy of 0.1K. The AVHRR data is acquired in three formats, namely high-resolution picture transmission (HRPT), local area coverage (LAC) and global area coverage (GAC). The average instantaneous field-of-view (IFOV) of 1.4 milliradians yields a LAC/HRPT ground resolution of approximately 1.1 km at the satellite nadir from the nominal orbit altitude of 833 km (Kidwell 1991). The GAC data are derived from an on board sample averaging of the full resolution AVHRR data, yielding 1.1-km by 4-km resolution at nadir. After TIROS-N NOAA-6 was launched in 1979 followed by consecutive launches (Hardman-Mountford 2000). In addition to the above, 'Pathfinder' data is also available at a spatial resolution of 9 km.

With the launch of the in 1981 of the European Space Agency's (ESA) Along Track Scanning Radiometer (ATSR) (ATSR 2000), a new source of radiometer data became operational. This was followed by the launch of ATSR-1 in 1991 on board the ERS-1 satellite and ATSR-2 in 1995 on board the ERS-2 satellite. Some of the specifications of ATSR include a spatial resolution of 1 km, an accuracy of  $\pm 0.3K$ , a self-calibrating system and a dual view design, which makes it possible to estimate and correct for atmospheric effects (ATSR 2000).

The biggest limitation of SST measurements from infrared sensors is probably the fact that it only measures the temperature of the upper few millimeters of the ocean, giving rise to the so-called skin effect. With passive sensor there is the additional

problem of cloud contamination, effectively reducing the spatial coverage of these sensors.

### **2.3.3 ERS SCATTEROMETERS**

The ERS-1/2 scatterometers measure radar backscatter from the ocean surface using three antennas that work in the C-band frequency (about 5.3 GHz). Wind vectors are estimated from the backscatter coefficients using semi-empirical models and inversion/dealiasing algorithms (Bentamy *et al* 1996 and Bentamy *et al* 1997). Vectors are initially provided at 50 km resolution with a separation of 25 km across a 500 km swath. Reconstruction of synoptic fields of surface winds on basin scales from discrete observations was achieved through statistical interpolation using the minimum variance method related to the Kriging technique (Bentamy *et al*, 1997). This provided the input for the estimation of weekly and monthly averages of the wind parameters over the global oceans into 1° by 1° squares.

Statistical comparisons with the National Data Buoy Center (NDBC), Tropical Atmosphere Ocean (TAO) and Japan Meteorological Agency (JMA) buoy wind measurements produced an rms error of approximately 1.20 m/s for wind speed and 24° for wind direction (Graber et al, 1996). More details on formulae and procedures used in estimating and validating the scatterometer and gridded data are contained in the literature cited.

Global accuracy of the gridded scatterometer wind fields is assessed through comparison with ECMWF analysis and Hallerman and Rosenstein (1983) and Florida

State University (FSU) wind stress climatologies. This yielded for example mean and standard deviation values of the difference between ERS and ECMWF wind field analyses of 0.53 m/s and 1.15 m/s for the wind speed, 0.22 m/s and 1.34 m/s for the zonal component, 0.05 m/s and 1.26 m/s for the meridional component. Large-scale differences were found in the Southern Hemisphere, introducing uncertainties regarding the accuracy of data used in analysis of the wind fields here. Unfortunately, this study does not include any statistical comparisons between the data in situ measurements in the study area, e.g. buoy measurements, and the scatterometer data used here.

Although scatterometer data only became available a number of years after that of infrared sensors, a large number of application already exist for this data, both in terrestrial and marine sciences.

### 3 MATERIALS AND METHODS

#### 3.1 STUDY AREA

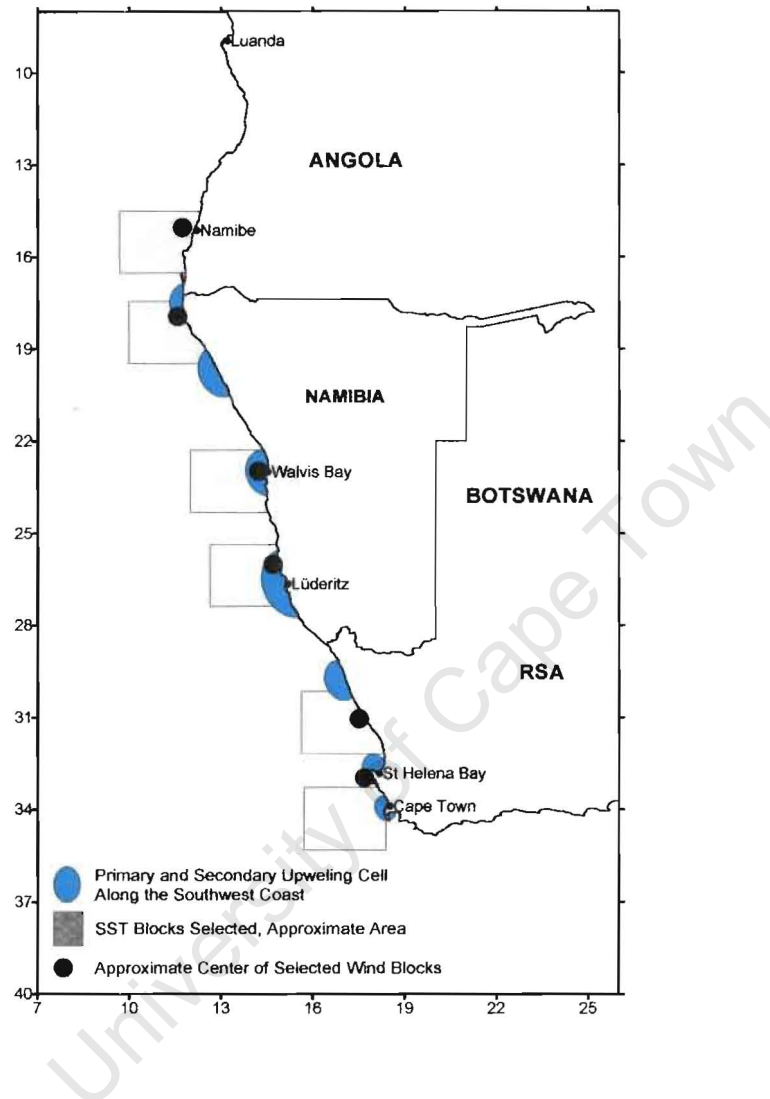


**Figure 6** The Major Area of Interest for this Study. Primary and Secondary Upwelling Cells have been Drawn after Shannon and Nelson (1996). Selections for the SST and Wind Analyses have also been drawn (see sections to follow).

The larger study area lies between  $0.5^{\circ}\text{E}$  and the coast and between  $0.5^{\circ}\text{S}$  and  $40.5^{\circ}\text{S}$ . Interpretation of results focused on a slightly smaller area of interest as mapped in Figure 6. It lies between  $7^{\circ}\text{E}$  and the coast and  $7^{\circ}\text{S}$  and  $40^{\circ}\text{S}$ . This covers the

whole of the Benguela upwelling region plus areas to the west, south and north of the region, thus constituting a large part of the South-East Atlantic. This was included as the Benguela is influenced from all three sides (Shillington 1998) and to give a broader spatial perspective of the conditions under investigation here. Sufficient attention has been given in the analysis to cover the entire study area. However, analysis on a finer scale has been done for the area adjacent to the coast as this is the area of greatest interest from the point of view of coastal upwelling.

## **3.2 DATA USED**

The study mainly focused on two aspects of the temporal variability of upwelling intensity and upwelling favorable conditions. These aspects are that of the variability at seasonal and inter-annual time scales. This is of course in addition to studying the spatial variability.

### **3.2.1 SEA SURFACE TEMPERATURE DATA**

Sea surface temperature (SST) data derived from in situ and satellite measurements were used to study the variability of upwelling (surface thermal properties) along the coast. One-degree gridded SST fields (Reynolds and Smith 1994) were used for analysis. Monthly SST fields were extracted for the period January 1982 to December 2000 to compile a 19-year dataset for analysis.

The analysis of the SST fields in the original dataset (data source) used in situ and satellite measured SST's as well as SST's simulated by the sea-ice cover (Reynolds 1988). The data was first adjusted for biases using the methods explained by

Reynolds (1988) and Reynolds and Marsico (1993). All analysis excluded land pixels and interpolation was done over ocean areas only. Optimum interpolated (OI) SST's are produced on a weekly basis (Sunday to Saturday) on a  $1^\circ \times 1^\circ$  grid. Monthly SST fields are derived by linear interpolation of the weekly fields to daily fields, which then are used to calculate the monthly averaged SST fields. More on the calculation of the optimum interpolation fields of SST can be found in Reynolds (1988), Reynolds and Marsico (1993) and Reynolds and Smith (1994).

### 3.2.2 WIND FIELDS

Scatterometer data from European Resources Satellites 1 and 2 (ERS 1 and 2) for the period January 1992 to December 2000 was analyzed to study the upwelling favorable conditions at the spatial and temporal scales mentioned earlier. Monthly averages of wind speed ( $W$ ), wind stress ( $\tau$ ) and the meridional ( $v$ ) and zonal ( $u$ ) components of the wind speed and wind stress were extracted for analysis.

Monthly averages of the wind fields were extracted from the Mean Wind Field Atlas on CD-ROM released by the Institut Francais pour l'Exploitation de la Mer (IFREMER). The gridded wind field was produced from scatterometer-retrieved wind vectors over the globe. Wind vectors are estimated from the backscatter coefficients of the measured radar backscatter of the ocean surface (Bentamy *et al*, 1997). Vectors are initially provided at 50 km resolution with a separation of 25 km across a 500 km swath. Reconstruction of synoptic fields of surface winds on basin scales from discrete observations was achieved through statistical interpolation using the minimum variance method related to the Kriging technique (Bentamy *et al*, 1997).

This provided the input for the estimation of weekly and monthly averages of the wind parameters over the global oceans into  $1^\circ$  by  $1^\circ$  squares.

### **3.3 DATA PROCESSING AND ANALYSIS**

Extraction of the wind data was performed with ExtrMWF.exe, an extraction program provided by IFREMER. Processing and analysis of the gridded SST and wind field data were done using the software packages Transform <sup>TM</sup>, Noeysys<sup>TM</sup> and Microsoft Excel <sup>TM</sup>.

Before any analysis was done, a land mask was applied to all data files. This was to ensure that further analyses excluded the land area. The land mask file was prepared by using a true color image from the original SST dataset. This was converted to a binary file and used to create the land mask, which was applied to both the SST and wind data files. The data points for the SST files were not changed as the same land mask was applied to the original data sets. With regards to the wind fields, this masking method was thought to be appropriate, as spatial conformity amongst the data sets would be achieved.

The wind field data used in this study contained a couple of problem areas, which had to be dealt with before any analysis could be done.

Firstly, no data was available for the month of February 1992. This problem was addressed by using the long-term average for February as a substitute for February 1992. It is believed that this did not change the end results significantly. Also,

having this long-term mean as an estimate is in any case better than having no estimate at all.

The second problem was that the components of the wind speed and wind stress provided are those directly in a north-south and an east-west direction. This of course is acceptable over the open ocean (Emery and Thomson 1998), but not at the coast where winds are topographically steered and altered. It is therefore desirable to resolve the vector components into alongshore components through the rotation (from Emery and Thomson 1998):

$$u' = u \cos\theta + v \sin\theta$$

$$v' = -u \sin\theta + v \cos\theta$$

This would provide estimates for the winds roughly parallel to the mean coastline. The wind stress vectors were rotated in the same way.

From Alan Boyd's (1987) estimation of the mean orientation of the coastline, which roughly runs from a SSE to a NNW direction, it was estimated that the components be rotated through an angle ( $\theta$ ) of about  $20^\circ$  in a positive counterclockwise direction (Figure 7). Although this was not the optimum for a number of known upwelling centers, it was thought to be a reasonable estimate for studying the larger scale features. This was also done to facilitate the easier calculation of the wind components for all data points along the coast.

As mentioned earlier, estimates for the wind components over the open ocean do not need to be rotated. These pixels however were included, for easier processing, and it is believed that the information deduced from their analysis would be representative enough of the overall conditions on the larger spatial scale. All analysis, unless otherwise indicated, that followed were done using the rotated components.



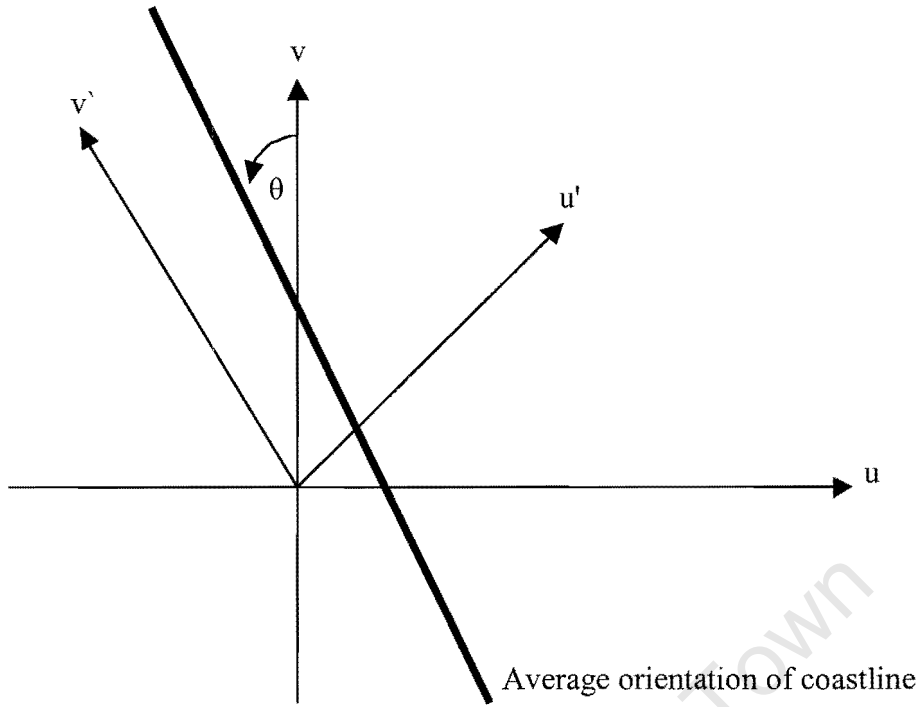


**Figure 7** Diagram illustrating how the rotation was done for the components of wind speed and wind stress

As it is mainly the alongshore components of the wind speed and wind stress that is of interest with regards to coastal upwelling, only these components together with the wind speed and wind stress magnitude were studied.

Since the original wind vector components were rotated before analysis, new wind stress vectors had to be calculated. These were calculated using standard formulae. Formulae used were (from Pond and Pickard 1983):

$$\tau_x = \rho_a C_D u (u^2 + v^2)^{1/2} \text{ N/m}^2$$

$$\tau_y = \rho_a C_D v (v^2 + u^2)^{1/2} \text{ N/m}^2$$

Where  $\rho_a$  is the air density taken as  $1.22 \text{ kg.m}^{-3}$  and  $C_D$  is the non-dimensional drag coefficient taken as a constant at 0.0013 (Kamstra 1985 and Johnson and Nelson 1999). The meridional and zonal wind-stresses are denoted by  $\tau_x$  and  $\tau_y$ .

During the data extraction in the analysis software, the data ranges provided in the documentation for each parameter was used to exclude land pixels right from the beginning. For the wind speed the range was between 0 m/s and 28 m/s. For the zonal and meridional wind speed components it ranged between -28 m/s and 28 m/s. That of the wind stress magnitude was between  $0 * 10^{-1}$  Pa and  $8 * 10^{-1}$  Pa and for the components of the wind stress it was between  $-8 * 10^{-1}$  Pa and  $8 * 10^{-1}$  Pa. Due to the fact that coastal pixels are normally contaminated as a result of the influence of landmasses, values for the parameters had to be estimated for the areas along the coast. This was done by interpolating, using kriging, for each parameter within the ranges given above. This was done for the entire area, including those pixels that would fall within the land. The pixels over the land were then masked out using the masking file discussed earlier. This would at least provide estimates for the area along the coast where it is of importance for coastal upwelling.

The following sections specifically deal with the processing and analysis done for studies at the required spatial scales.

### **3.3.1 SST FIELDS**

Mean monthly SST climatologies for the study area were computed from the monthly averaged SST fields. The twelve mean monthly images of SST were used to interpret the mean seasonal patterns of the SST fields. Attention was given to the mean seasonal distribution of sea surface temperature, the changes of this distribution between seasons and the spatial changes within and between seasons.

The first three pixels adjacent to the coast (about 180 miles) were then extracted for each month during the study period, and a zonal area average SST calculated. This was used to derive mean monthly SST's at the coast, which was then plotted as a Hovmuller diagram and as a function of latitude and time. It was expected that results from this exercise would yield slightly more information on the seasonal changes of SST along the coast.

The monthly and mean monthly SST's were used to calculate the SST anomalies at the coast. This was again plotted as latitude versus time. SST anomalies were defined as the deviations of the monthly SST from the mean monthly SST for a particular month. The main purpose for this was to aid in identification of anomalous periods/years during which the SST deviations from the mean was either abnormally high or low.

For enhanced interpretation, the SST's for six  $2^{\circ} \times 2^{\circ}$  blocks at various locations along the coast and for each month in the data set, were extracted. Their positions follow below (See Figure 6).

Block 1 –  $14.5 - 16.5^{\circ}\text{S}$  and  $9.5 - 11.5^{\circ}\text{E}$  (Southern Angola)

Block 2 –  $17.5 - 19.5^{\circ}\text{S}$  and  $9.5 - 11.5^{\circ}\text{E}$  (Northern Namibia)

Block 3 –  $22.5 - 24.5^{\circ}\text{S}$  and  $11.5 - 13.5^{\circ}\text{E}$  (Central Namibia)

Block 4 –  $25.5 - 27.5^{\circ}\text{S}$  and  $12.5 - 14.5^{\circ}\text{E}$  (Southern Namibia)

Block 5 –  $30.5 - 32.5^{\circ}\text{S}$  and  $15.5 - 17.5^{\circ}\text{E}$  (Northwest South Africa)

Block 6 –  $32.5 - 34.5^{\circ}\text{S}$  and  $15.5 - 17.5^{\circ}\text{E}$  (Southern South Africa)

These areas were selected in a way that it is representative of major coastal regions in the system. It was further attempted to select sites in such a way to fall within or close to known upwelling cells along the coast.

For each of these blocks, an area average SST per month was calculated and used to calculate the monthly SST climatologies and SST anomalies. This enhanced the identification of seasonal patterns at each location, and further improved the ability to compare the different areas along the coast with each other.

The above results were jointly used to study the seasonal and inter-annual variability of the SST's along the coast and to identify anomalous events as they occurred during the study period. It also provided information on the spatial extent of the SST variability, particularly with regards to the frequency and intensity of identified anomalous events. These results provided a further opportunity to compare different regions in the system with each other with regards to the occurrence of anomalous events.

### **3.3.2 WIND FIELDS**

Monthly averaged data for the absolute wind speed and stress, and the computed northerly components of the wind speed and wind stress were used to compute mean monthly images for each parameter. Twelve mean monthly images of each of the parameters were prepared in the same manner as discussed in the previous section. Visual interpretation of these yielded information on their spatial and temporal variability within and between the seasons.

Similar to what was done with the SST fields, an extraction was performed on the first three pixels next to the coast, a zonal average calculated and plotted as a function of

latitude and time. Mean monthly images were computed from the extracted monthly data and plotted as a function of latitude over time. This was done to see if it could improve the ability to resolve seasonal and latitudinal changes more easily.

For refined interpretation, six coastal pixels ( $1^{\circ} \times 1^{\circ}$ ) of the upwelling favorable wind stress were extracted at similar locations as the SST blocks. The location of these pixels was chosen to approximately coincide with that of the selected sites in the SST analysis for the same reasons as mentioned in previous discussions. Their positions were determined at: **15 °S, 23 °S, 26 °S, 31 °S, and 33 °S** (See Figure 6). For each location, the mean monthly values were computed and plotted together with the monthly estimates of the alongshore wind stress.

Results from both analyses were used to study the seasonal and inter-annual variability of upwelling favorable conditions over the study area. Furthermore, its applicability in identifying anomalous events was investigated. Results were also used in combination to study the latitudinal variations in upwelling conditions along the coast.

### 3.3.3 UPWELLING INDICES

#### 3.3.3.1 SST Upwelling Index (SST UI)

Upwelling along the coast causes cooler sub-surface water to rise to the surface. This usually have the result of cooler upwelled water close to the coast with the warmer, more oceanic waters at some distance offshore (Nykjær and Van Camp 1994). This provided the basis for defining the SST Upwelling Index (SST UI) used here as the zonal temperature difference between a pixel at the coast and that at some distance offshore. The same approach has been followed by, amongst other, Nykjær and Van Camp (1994). The distance of the offshore pixel was taken at about 700 miles from the coast to minimize the possibility of including upwelled waters entrained in an offshore moving upwelling filament. The formula used here was:

$$\text{SST UI} = \text{SST}_{\text{coast}} - \text{SST}_{\text{offshore}}$$

A negative difference would suggest cooler waters at the coast. A higher negative value would then suggest more intense upwelling at the coast. Positive differences would suggest warmer waters at the coast and upwelling is then assumed to be quiescent or absent at the time. Small differences in SST would suggest uniform warming both inshore and offshore and would probably also suggest very limited or no upwelling at the time.

SST Upwelling indices were calculated for each month. The monthly index was used to derive a mean monthly index and both were plotted as a function of latitude and time. It was further hoped that results would either confirm or add to the interpretations made from the SST fields as discussed in the previous sections.

### 3.3.3.2 Ekman Upwelling Index

Since upwelling is attributed mainly to the force exerted by the alongshore component of the wind stress and the rotation of the earth (Nykjær and Van Camp 1994), an upwelling index was calculated using this component of the wind stress. It is calculated as the Ekman transport perpendicular to the coast, similar to what Johnson and Nelson (1999) did for the Cape Columbine area using winds measured at the lighthouse there. The Ekman transport was calculated for each of the ( $1^\circ \times 1^\circ$ ) selected sites mentioned earlier and are given by:

$$S_x = \tau_y / |f|$$

This gives a value of kilograms of water per meter of coastline per second [kg/m/s]. Each block is 1 degree long (about 60 miles or 111 km). Thus, dividing the Ekman Transport [ $S_x$ ] by the density of seawater and multiplying it by 111 km (or 111 000 m), gave the total volume of offshore transport along the coast per block [ $\text{m}^3/\text{s}$ ]. These were plotted on a monthly scale for the investigation of both inter-annual and latitudinal variability. Mean monthly plots for each block was computed to obtain the mean volume transport for each season. Comparisons were made in the same way as discussed in the previous sections.

## 4 RESULTS AND DISCUSSION

### 4.1 SEASONAL VARIABILITY

#### 4.1.1 WIND CONDITIONS

##### 4.1.1.1 Southerly winds and wind stress

The mean monthly meridional wind speed for the entire area is plotted in Figure 8 whereas that at the coast is plotted in Figure 9. In Figures 9 and 10 the mean monthly meridional wind stress along the coast and for the entire study area are plotted respectively. Results shown in these figures compare well with that of other works on the prevailing wind condition over the system.

Similar to what was found by, amongst others, Parish *et al* (1983) and Bakun and Nelson (1991), results here suggested that although upwelling favorable winds occur along most of the coast south of 16 °S throughout the year, seasonal and latitudinal variations in the wind field do occur. Between 16 °S and 29 °S, the highest wind speeds are found for most of the year, with mean speeds ranging between 4 m.s<sup>-1</sup> and 7 m.s<sup>-1</sup>. North of 16 °S wind speeds are generally very low and less variable with little or no wind induced upwelling expected.

A wedge-shape feature of strong southerly winds is present throughout most of the year. This feature extends offshore and in a northwesterly direction and intensifies during autumn and winter. It is more contracted during spring and summer. Bakun and Nelson (1991), through the analysis of the wind stress curl over the region, also reported on the existence of this feature. Like in Parish *et al* (1983) and Kamstra



(1985) it was found here that the highest wind stress is normally found some 200 – 300 km offshore. This give rise to a cross-shore gradient in wind speeds for most of the area, with wind speeds increasing in an offshore gradient. This is particularly evident along the central Namibian coast near Walvis Bay.

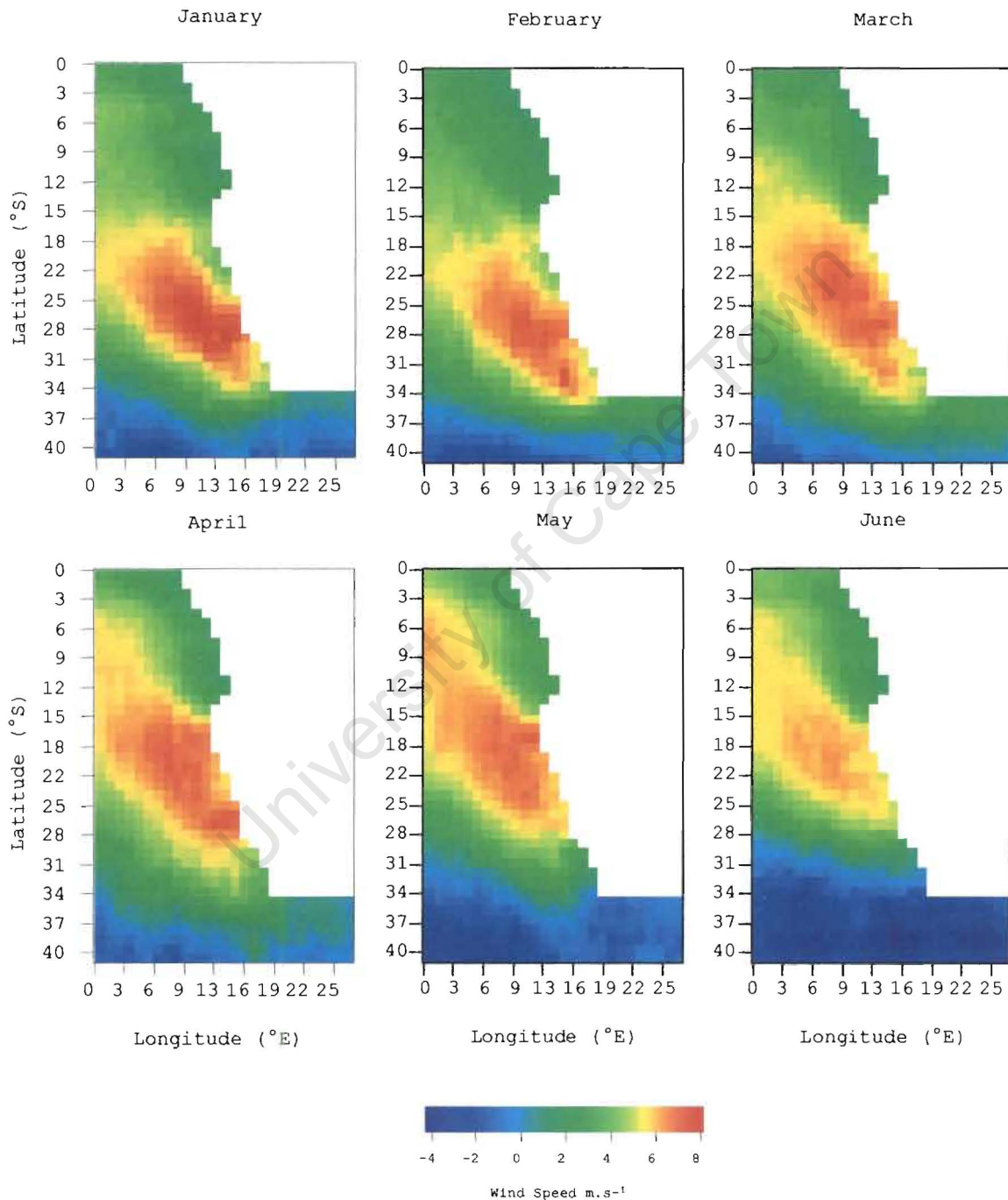


**Figure 8:** Mean Monthly Meridional Wind Speed for Study Area

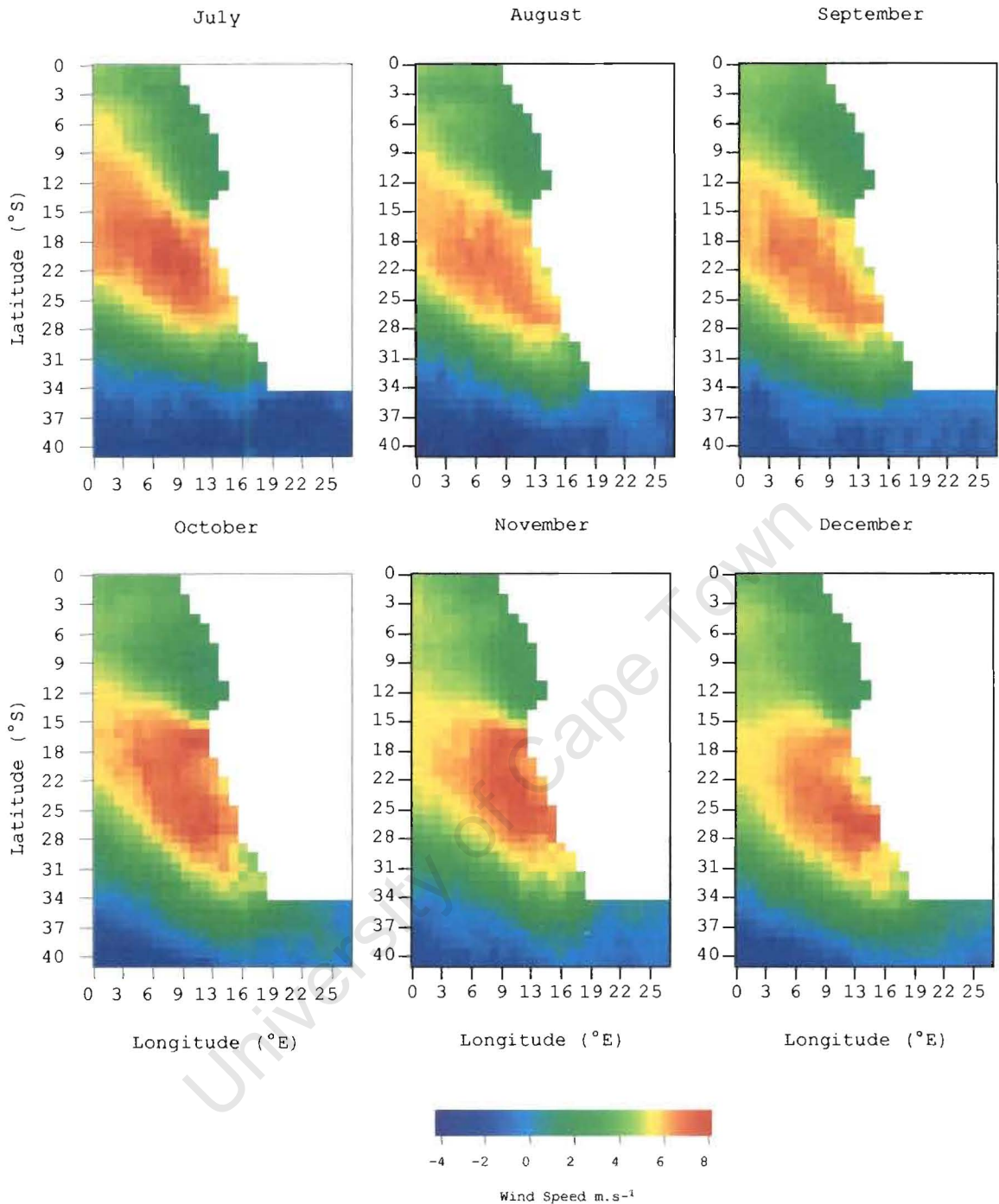


**Figure 8 (contd.):** Mean Monthly Meridional Wind Speed for Study Area

Figures 8, 9 and 10 suggest that the area around Lüderitz ( $\sim 25^{\circ}\text{S} - 27^{\circ}\text{S}$ ) is experiencing the strongest upwelling favorable winds ( $2.5\text{m.s}^{-1} - 7.5\text{m.s}^{-1}$ ) throughout the year. With the highest equatorward wind stress found here for most of the year, it is suggested that this region is probably the most prominent cell of potential

upwelling along the coast. There is however a slight slackening in these equatorward winds between May and July.

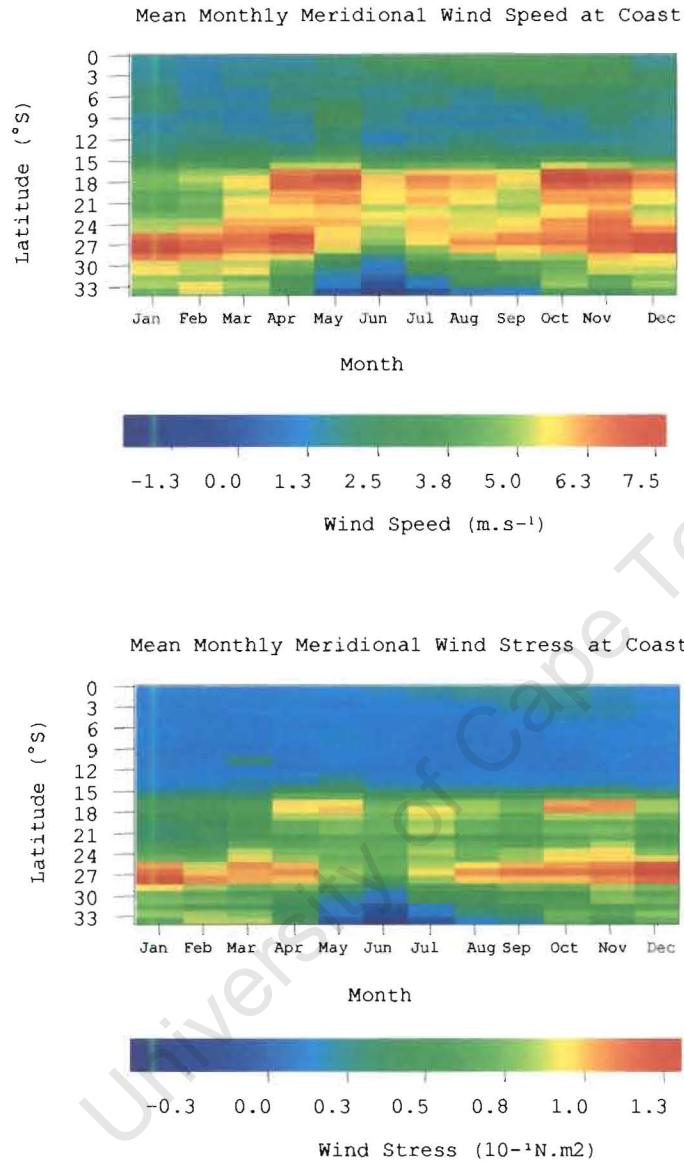


**Figure 9:** Mean Monthly Meridional Wind Speed and Stress at the Coast

In the north ( $\sim 18^\circ \text{S}$ ) near Cape Frio, a secondary cell of potential upwelling can be observed with maxima in the wind stress experienced in April/May, July and October/November. During these months strong winds ( $> 6 \text{ m.s}^{-1}$ ) prevails over this area.

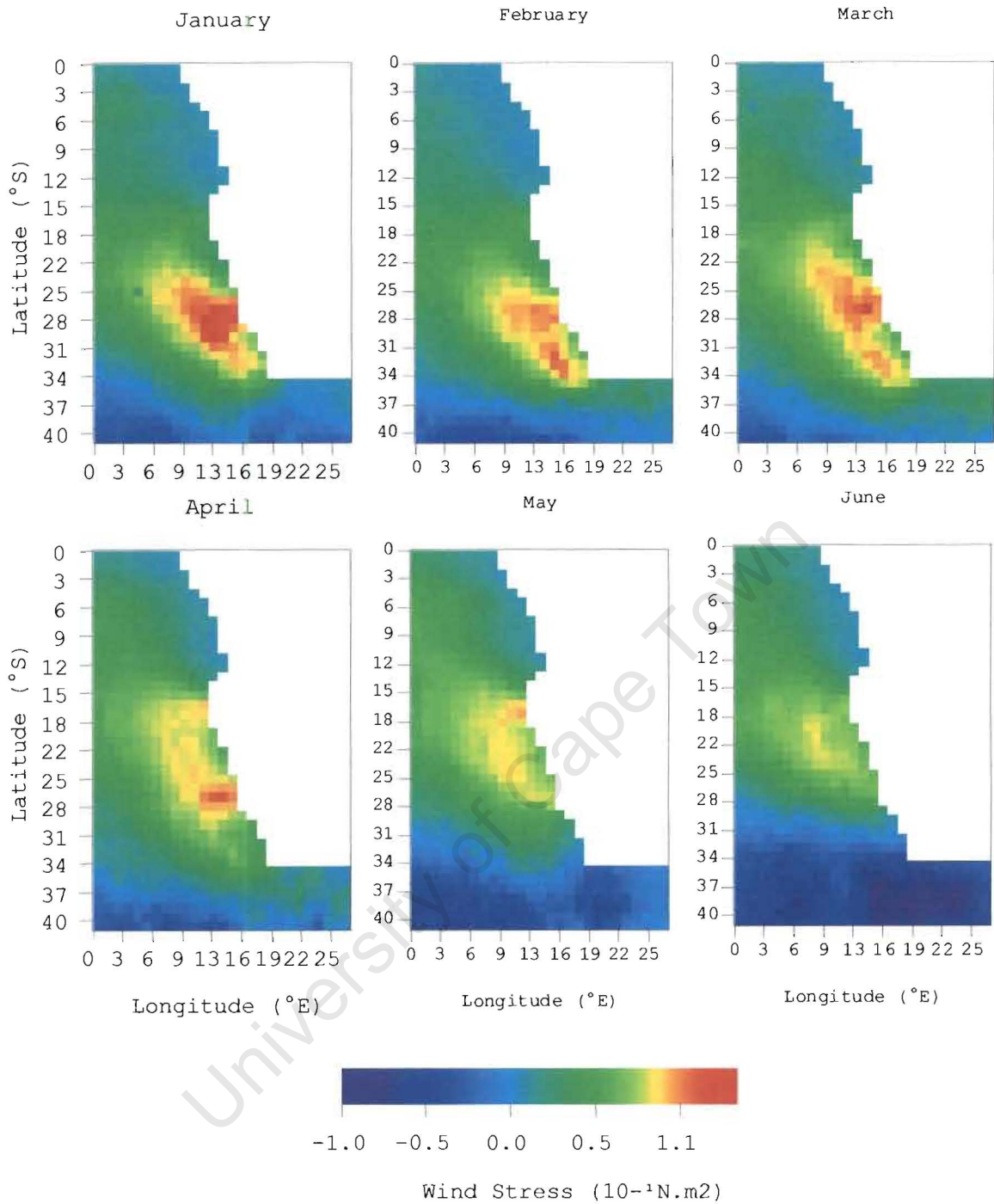


**Figure 10:** Mean Monthly Meridional Wind Stress for Study Area

Along the central Namibian coast, between Cape Frio and Lüderitz, upwelling favorable winds also appear to be present throughout the year. Wind speeds are however generally and less variable, and range between approximately  $4 \text{ m.s}^{-1}$  and  $5 \text{ m.s}^{-1}$ .



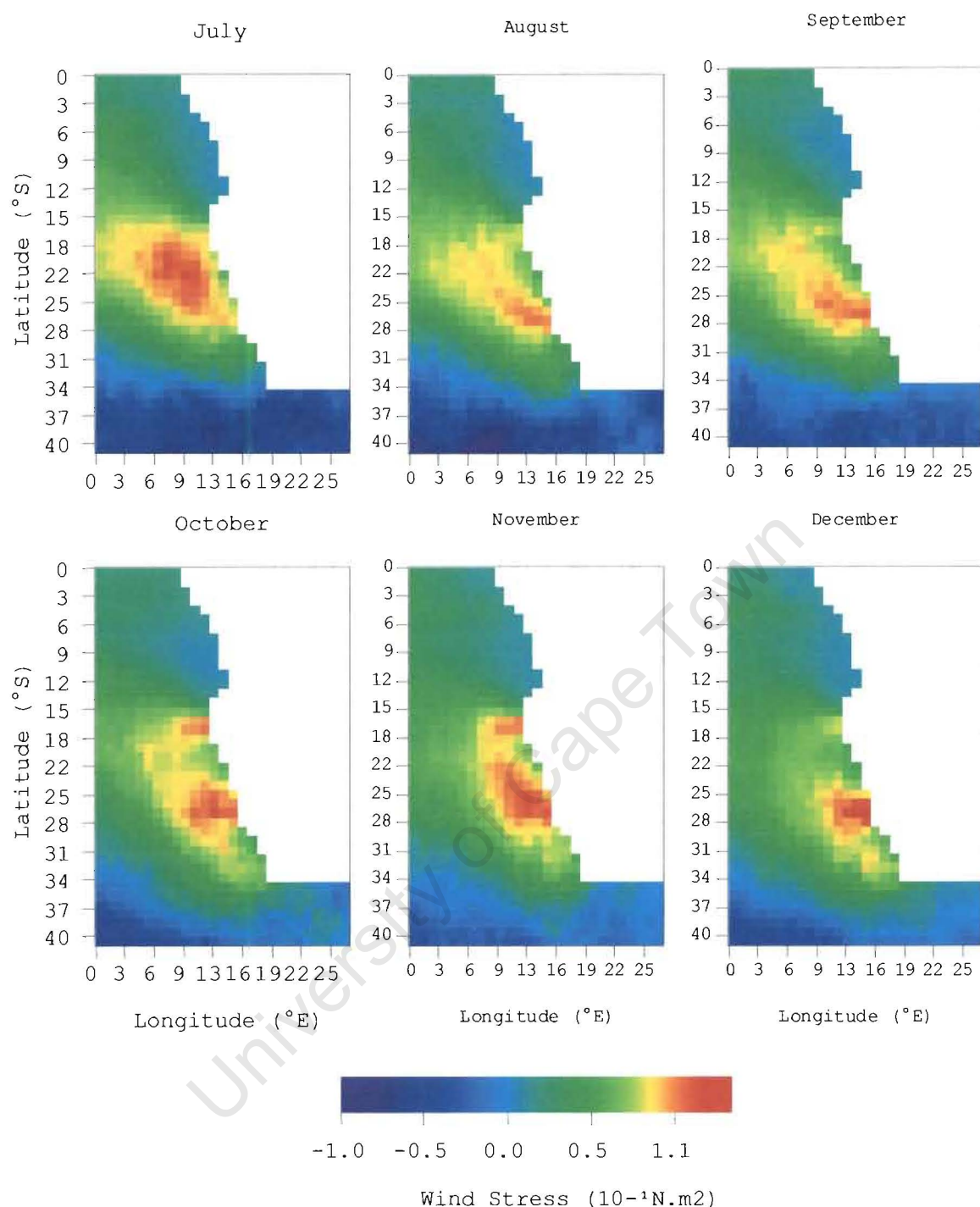


**Figure 10 (contd.):** Mean Monthly Meridional Wind Stress for Study Area

In the south (30 °S – 34 °S), the strongest southerly winds appear to be blowing during spring and summer (2.5 m.s<sup>-1</sup> - 6 m.s<sup>-1</sup>). Near Cape Columbine and the Cape Peninsula in the south (~ 32 °S) upwelling favorable condition (southerly winds) are generally less intense than the potential upwelling cells further north in the system.

Between May and July upwelling favorable conditions are completely absent. These areas can be described as summer upwelling cells as upwelling would mainly occur during spring and summer.

#### **4.1.1.2 Ekman Upwelling Index (EUI)**

The seasonal distribution of upwelling conditions at the selected sites are depicted in Figure 11 and 12, which are the monthly means of the Ekman Upwelling Index or total volume transport and the mean monthly alongshore wind stress per  $1^\circ$  block. Seasonality along the coast is clearly varying. It would appear that a stronger seasonal signal is observed towards the latitudinal ends of the study area. In the north ( $15^\circ\text{S}$  and  $18^\circ\text{S}$ ) clear peaks are reached during April/May and October/November with the volume of the offshore transport per block just less than  $0.2\text{ Sv}$ . A summer minimum is evident between December and February ( $< 0.15\text{ Sv}$ ). Minima are also observed during the months between June and September. Along the central Namibian coast ( $23^\circ\text{S}$ ) seasonal variations are generally smaller. Slight maxima do however occur during March, July and November with minima during the months from December to February. At Lüderitz ( $26^\circ\text{S}$ ) upwelling is at its weakest during June (winter). Offshore transport (upwelling) here remains significant though throughout the year, as in the case of the other sites further north. In summer, total volume transport at Lüderitz can be over  $0.2\text{ Sv}$ . At the two southern sites ( $31^\circ\text{S}$  and  $33^\circ\text{S}$ ) upwelling completely ceases during the winter months. A very pronounced seasonal signal is observed with peak upwelling during late spring and summer. Mean transport in summer is suggested to be roughly around  $0.1\text{ Sv}$  at its peak.

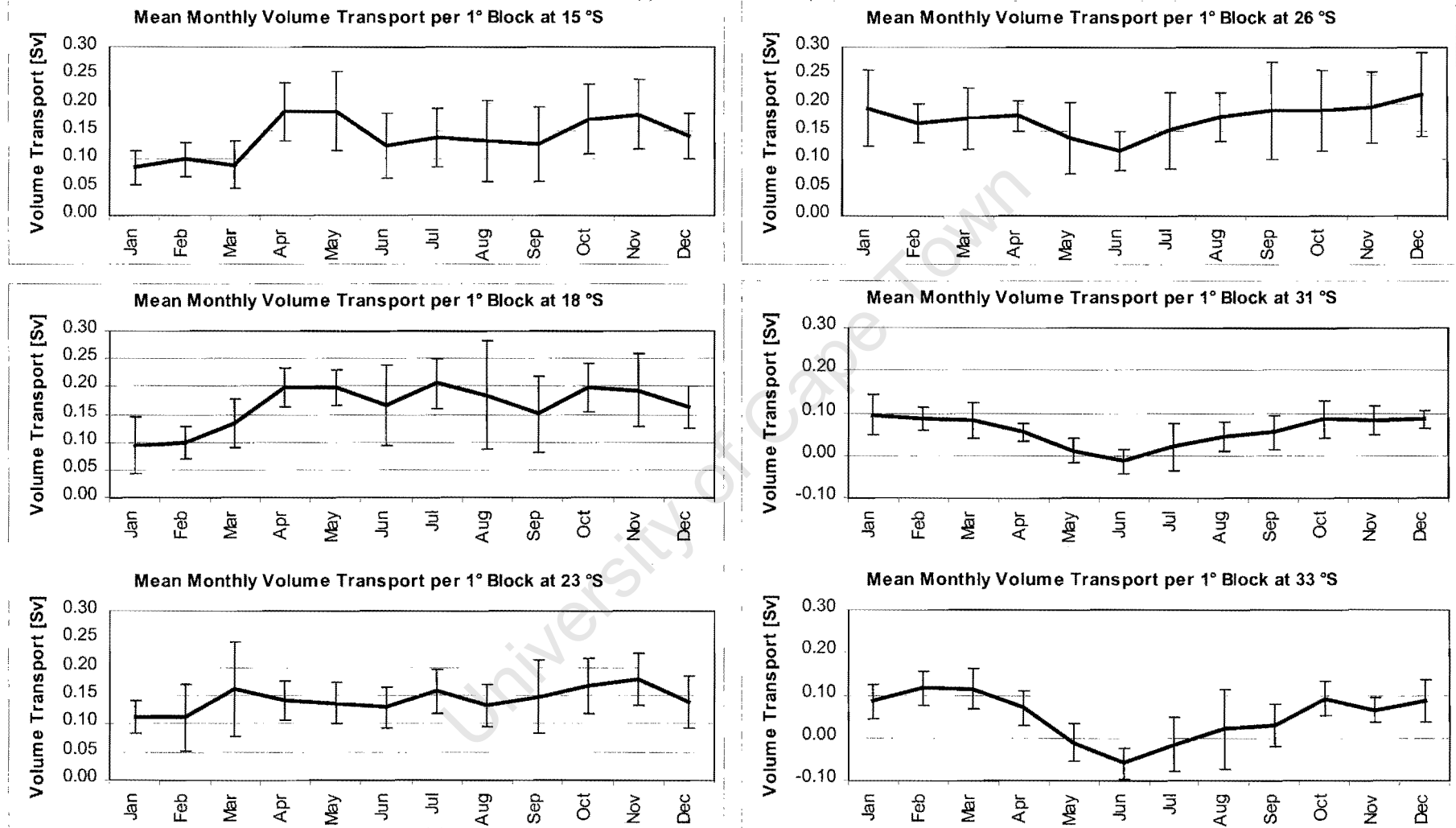


**Figure 11:** Mean Monthly Volume Transport at Selected Sites with Standard Deviations

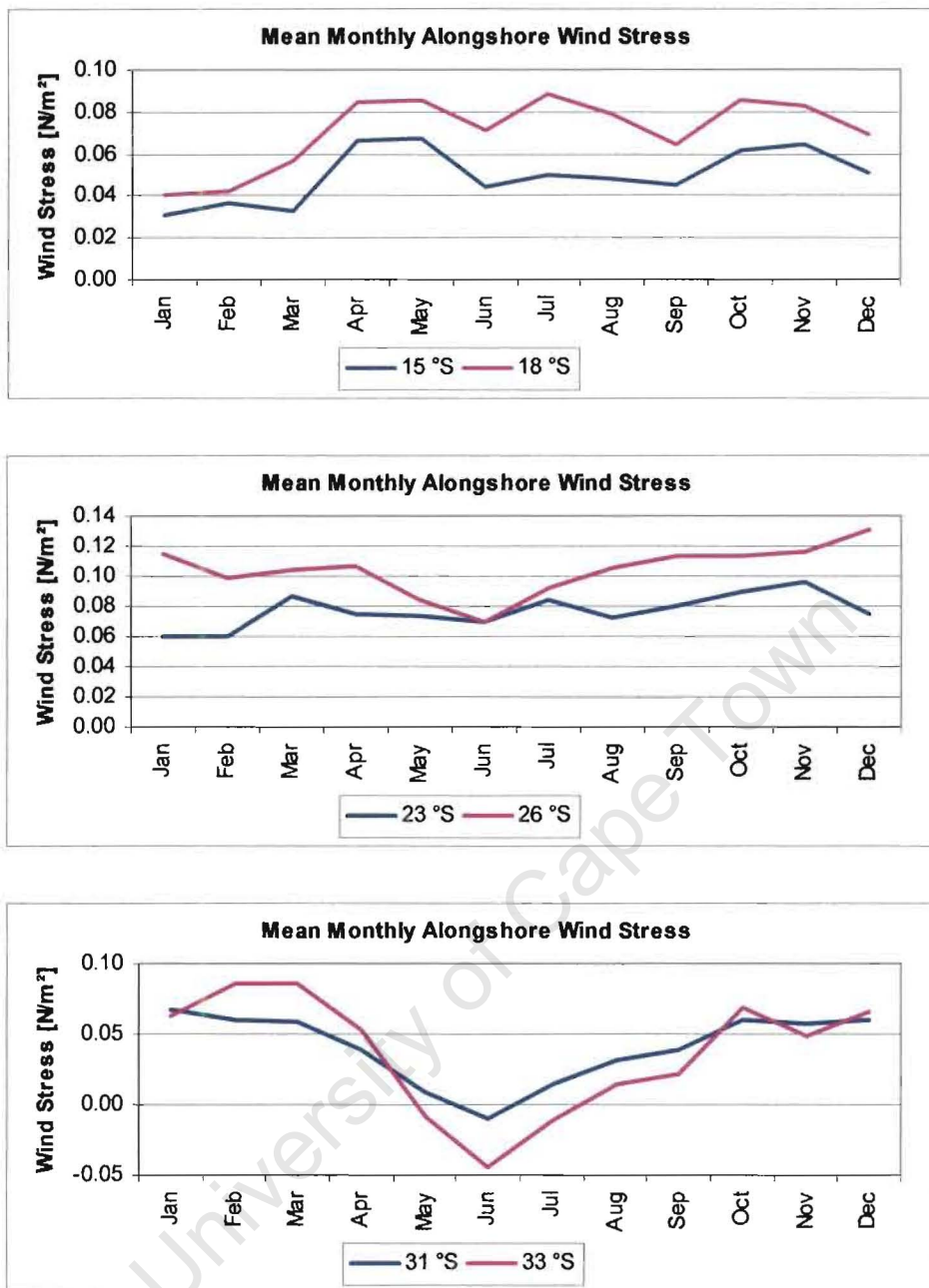


**Figure 12:** Mean Monthly Meridional Wind Stress at Selected Sites

The identification of the major upwelling cell at Lüderitz, a secondary cell at Cape Frio and the summer upwelling cells at the Cape Peninsula is well in accordance with findings by amongst others, Parrish *et al* (1983) and Boyd (1987). The seasonality of the South Atlantic High Pressure System and the resultant upwelling conditions have been discussed by numerous authors. These include works by Nelson and Hutchings (1983), Kamstra (1985), Shannon (1985), Boyd (1987), Preston-Whyte and Tyson



(1988), Hutchings and Taunton-Clark (1990), Shannon and Nelson (1996); Shillington (1998) and Johnson and Nelson (1999). Findings from this study agrees well with that discussed by these authors, thus confirming the relevance and applicability of the data used here.

University of Cape Town

#### 4.1.2 SEA SURFACE TEMPERATURE

The mean monthly SST imagery (Figure 13) suggests a relatively clear cycle of warming and cooling throughout the year. Significant warming appears to have an onset during October (mid-spring) after which the entire system appears to become progressively warmer. This ultimately peaks during February to April (late summer/autumn) when the highest SST's are observed. Cooling of the system starts to set in during May, with the lowest SST's observed during July and August (winter). In general, seasonal warming appears to be moving in from the north and northwest, pushing southward until it start retracting during May. On the other end, cool water seems to approach from the southwest during May/June. Its most northward influence appears to be reaching as far north as 18 °S.

Latitudinal differences in SST appear to be more pronounced than those in an east-west direction. It is evident that the highest SST's are found in the north of the study area, with the coolest SST's evident in the south and especially southwest of the sub-continent. The region in between (roughly between 17 °S and 34 °S) shows more moderate temperatures. The variability here generally seems less than that at the latitudinal extremities of the study area. SST's does not generally change sharply in the longitudinal direction. This is especially the case when the area is taken as that extending directly from the coast offshore.

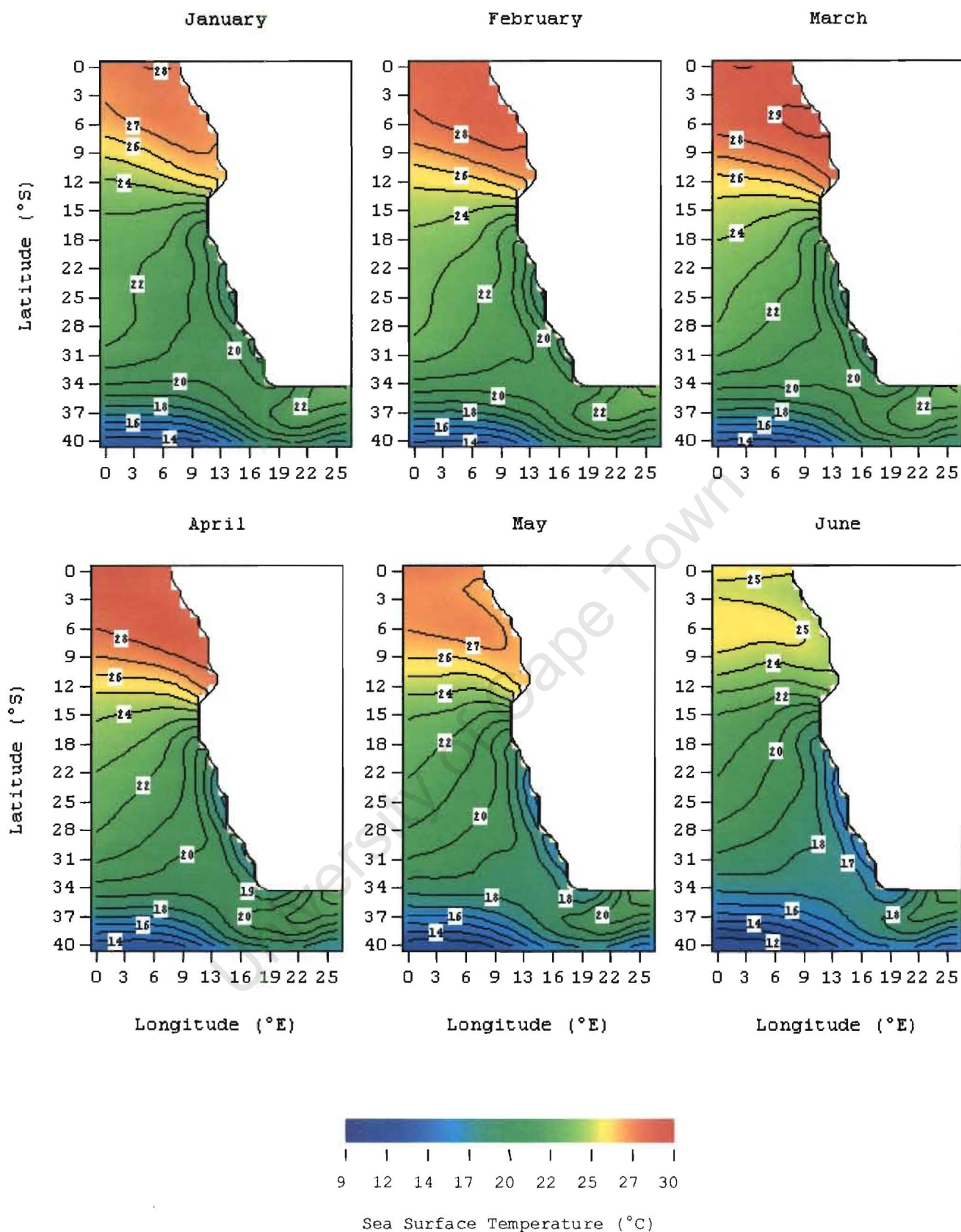


**Figure 13: Mean Monthly SST for Study Area**

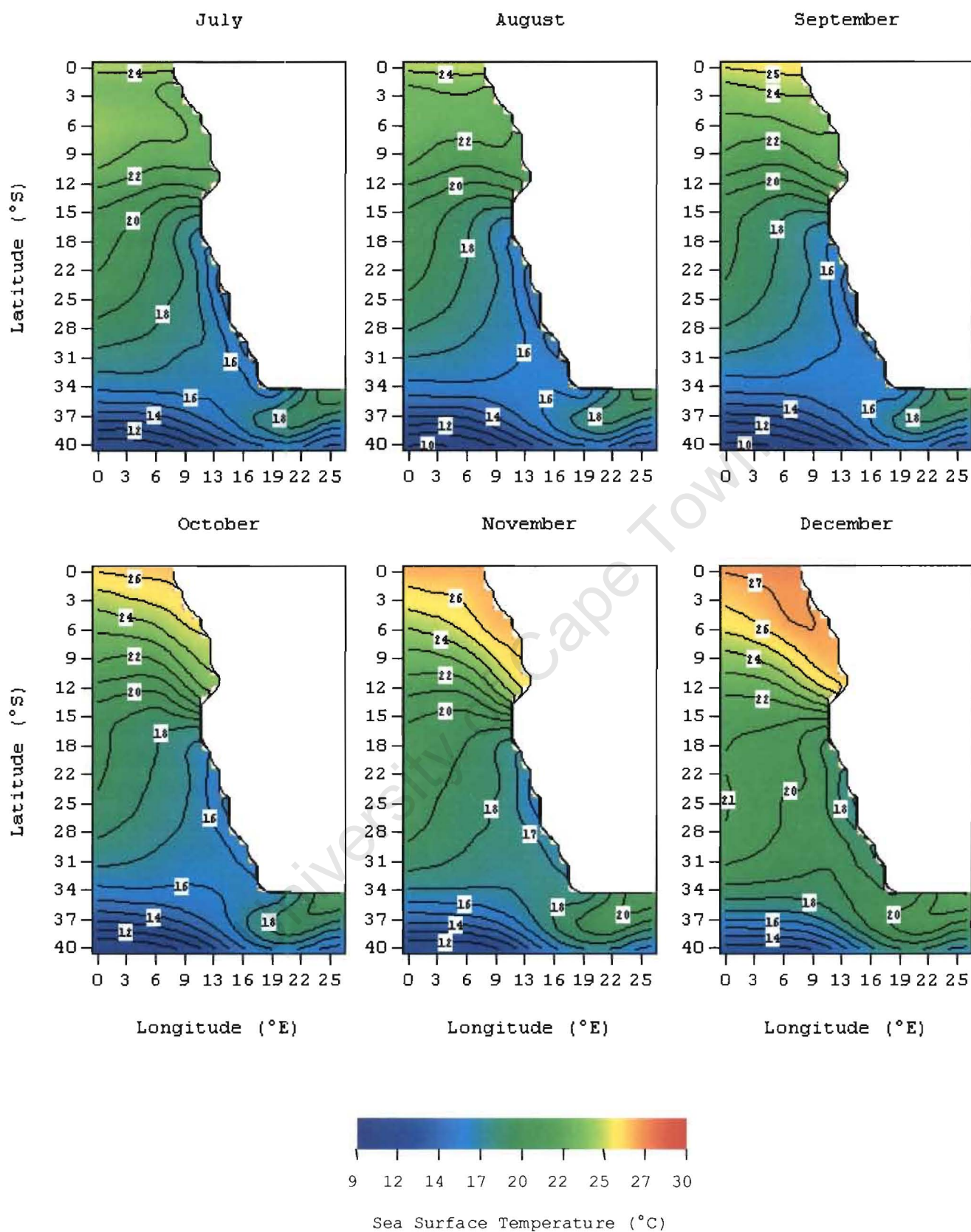


**Figure 13 (contd.):** Mean Monthly SST for Study Area

The major interest of this thesis is of course those conditions prevailing at the coast and its associated variability. Figure 14 is a Hovmuller diagram of the mean monthly SST at the coast as extracted and computed from the original monthly SST data. From the study of this diagram one concludes that there appears to be five (5) distinct latitudinal zones with each having a different seasonal SST pattern.

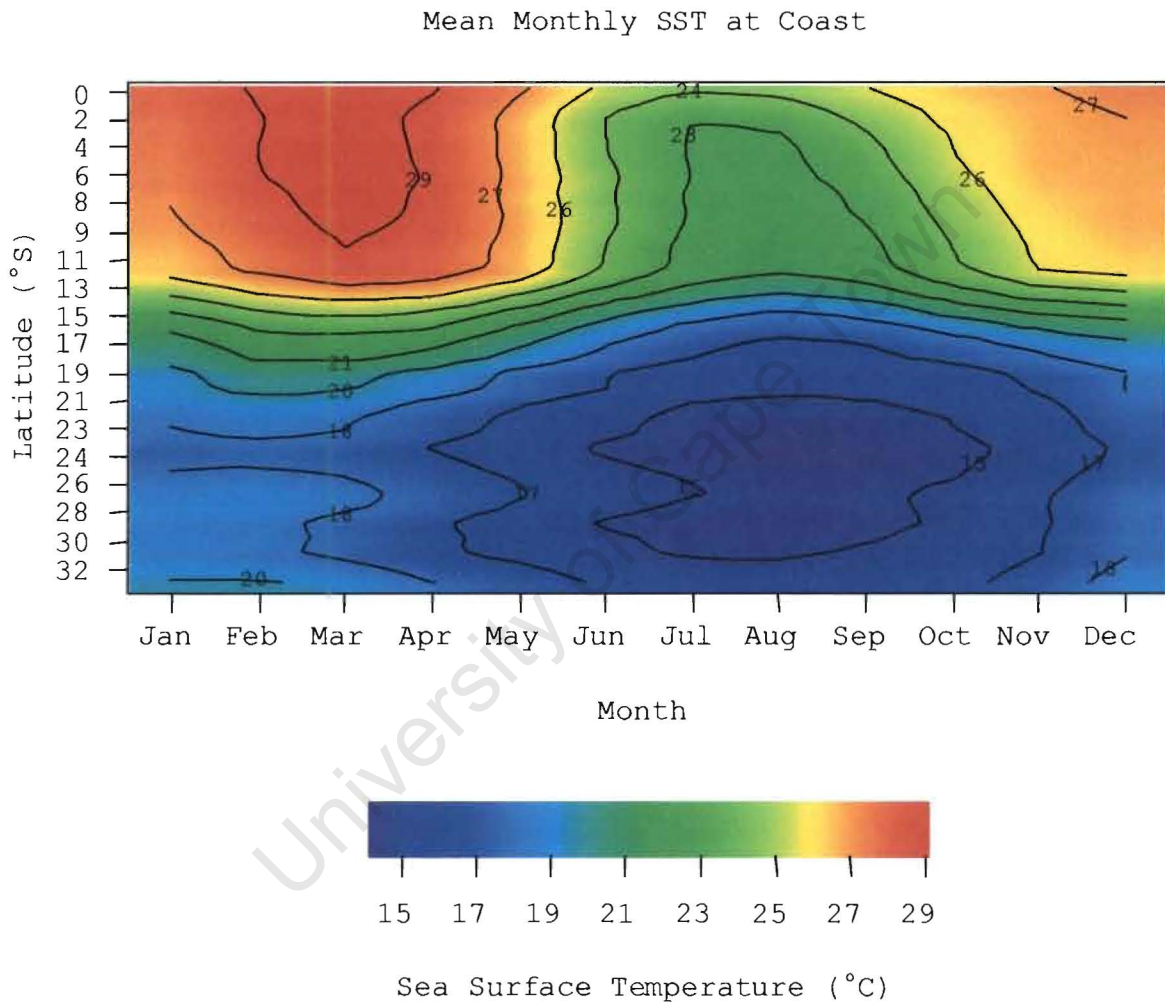


**Figure 14:** Mean Monthly SST at Coast

The first zone that can be identified lies north of 13 °S. This zone shows the highest mean SST's at any time with mean SST's almost always higher than 23 °C. It has a very clear seasonal cycle with cooler temperatures generally experienced between



mid-May and mid-October. Warming starts again during September/October and lasts until April/May. The highest SST's ( $>29^{\circ}\text{C}$ ) are observed between February and April. Persistent warm conditions here is probably due to the combined effects of the area's close proximity to the equator, thus receiving large amounts of solar heating throughout the year, and the presence of the warm southward flowing Angola current, transporting and maintaining warm waters in this region.

A second, zone can be identified roughly between  $13^{\circ}\text{S}$  and  $18^{\circ}\text{S}$ . This area remains relatively warm throughout the year. However, slight cooling takes place during winter. Isotherms are generally close to each other suggesting a sharp temperature gradient between  $26^{\circ}\text{C}$  at the northern boundary and  $20^{\circ}\text{C}$  at the southern boundary for most of the year except during winter. The close isotherms suggest the presence of a possible semi-permanent thermal frontal zone. According to Shannon *et al* (1986) these latitudes approximately coincide with that of the mean position of the Angola-Benguela Frontal Zone (ABFZ). Although the temperature gradients may not be as sharp as described in other literature, results suggest that this area be that of the ABFZ. This is despite the fact that the coarse spatial resolution of the data to some extent smoothes out the temperature gradients observed.

A third zone was identified between  $18^{\circ}\text{S}$  and  $22^{\circ}\text{S}$ . Similar to findings by Boyd (1987) and Cole (1997), this zone is characterized by moderate temperatures ( $15^{\circ}\text{C}$  -  $21^{\circ}\text{C}$ ), which do not change too much between seasons. A cool winter period ( $<15^{\circ}\text{C}$  and  $20^{\circ}\text{C}$ ) are followed by slightly higher SST's between December and May. Seasonal heating here as very characteristic of that at the mid-latitudes. The effects of

coastal upwelling on the SST patterning here are much more pronounced as in the zones further north (see previous section).

The fourth, zone lies between 20 °S and 27 °S. SST's generally range between <15 °C and 20 °C. Although slight warming can be observed between December and March (18 – 20 °C), SST's are rather low and constant throughout the year. The effects of this seasonal warming seem to be rather limited in the area between 23 °S and 27 °S. The effects of winter cooling can be seen in the entire zone between May and September. Here, persistent upwelling plays an even greater role in the coastal SST's (Cole 1997).

The fifth and southernmost zone lies south 27 °S. Seasonality is similar to seen in the third zone described above. The highest SST's are normally experienced between December and March/April with mean SST's around 19/20 °C. This is despite the fact that relatively strong summer upwelling occurs in this region.

In general, from Figure 14, the lowest SST's (15 °C or less) are observed between June and October, and then for the area between 22 °S and 31 °S. Lüderitz and surroundings are seen to be the coolest for most of the year.

Figure 15 is a diagram of the mean monthly SST at each of the selected areas discussed earlier. Results obtained from analyzing these plots yielded similar results to that of the Hovmuller diagram discussed in the previous paragraphs. There is however a few remarks that needs mention at this stage. It is clear that seasonal differences in SST in the north (Southern Angola and Northern Namibia – 15 and 18

°S) are generally larger than the rest of the selected sites. The seasonal differences become progressively smaller further southward. It is only at the most southerly site (33 °S) that the seasonal difference becomes slightly larger again. In general, the highest SST's at all sites occur during mid-summer to autumn (January – April) with the lowest SST's observed during August/September (late-winter/early-spring).

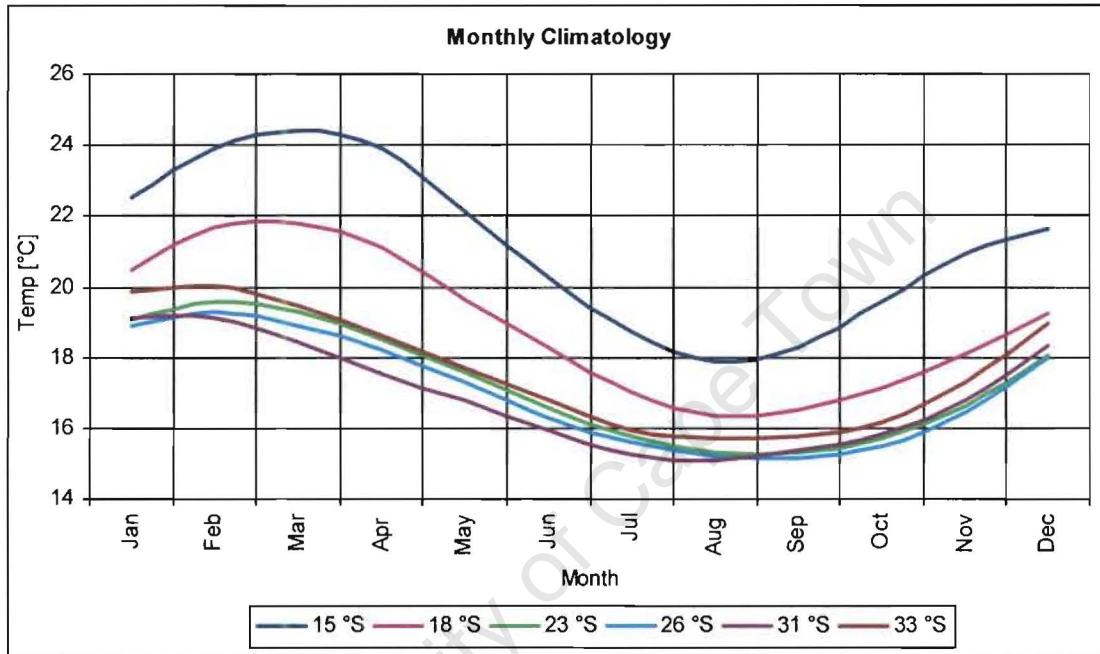


**Figure 15:** Mean Monthly SST at Selected Sites

Although SST's are probably influenced by the seasonal cycle of solar heating, it is expected that cooling due to upwelling also play a significant role. Similar seasonal patterns in the wind fields and SST's are described in the literature discussed and cited in Chapter 2. These include Nelson and Hutchings (1983), Shannon (1985), Boyd (1987), Shannon and Nelson (1996), Cole and McGlade (1998) and Shillington (1998).



## 4.2 INTER-ANNUAL VARIABILITY

### 4.2.1 WIND CONDITIONS

The inter-annual variability of the upwelling favorable conditions at the coast was studied using both the computed Ekman transport and the anomalies of the upwelling favorable wind stress (southerly wind stress) and the Ekman Upwelling Index (EUI).

The alongshore wind stress anomalies at the coast are plotted as a Hovmuller diagram in Figure 16 as a function of latitude and time (years). Most of the variability observed in Figure 16 appears to be related to the seasonal variability from year to year. Anomalies generally seem weak, especially north of 14 °S. The most pronounced positive anomalies for the coastal area further south appear to have occurred between the autumn of 1998 and the summer of 1999 when stronger than usual alongshore winds appear to have prevailed. Weaker winds are observed for the summers of 1996 and 1998 for most of the region except for that area north of 14 °S.

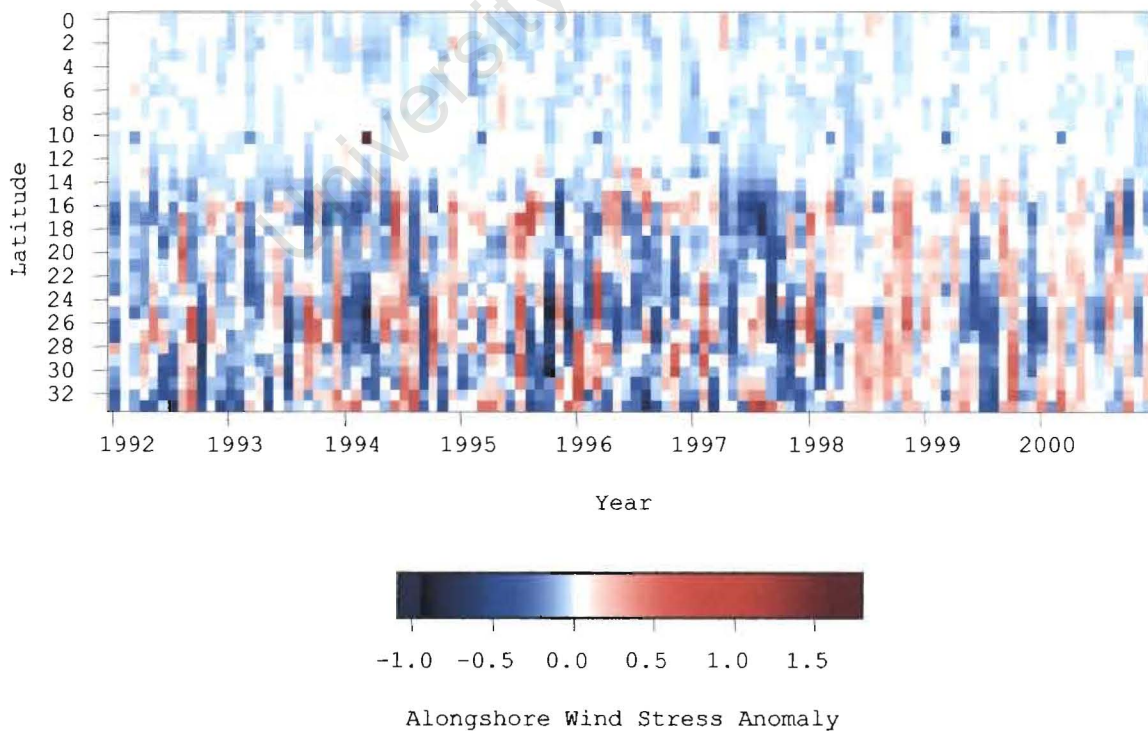


**Figure 16:** Anomalies of the Alongshore Wind Stress at the Coast

To enhance the interpretability of the wind stress and transport anomalies, these were calculated for each of the six sites and plotted over time (Figure 17). The table below gives a summary of the anomalies identified at these sites. Only the strongest anomalies are highlighted with a plus sign indicating a positive anomaly and a minus sign indicating the opposite. Possible significant anomalies were derived using the averages of the deviation from the mean of the alongshore wind stress at each site. Values larger or smaller than these were classed as either positive or negative anomalies. The cut-off values for each site was determined to be as follows:

15 °S – 0.018 N/m<sup>2</sup>; 18 °S – 0.022 N/m<sup>2</sup>; 23 °S – 0.021 N/m<sup>2</sup>; 26 °S – 0.030 N/m<sup>2</sup>

31 °S – 0.027 N/m<sup>2</sup>; 33 °S – 0.044 N/m<sup>2</sup>

From Figure 17 there are indications of a significant negatively anomaly was in the northern Benguela between October and December 1995. A longer, more persistent negative anomaly was experienced during July and November 1997 in the northern Benguela. It was especially evident between September and November 1997 in the vicinity of Lüderitz (26 °S). This was surprising as 1997 is generally considered amongst local scientists to have been a rather cool year, especially in the northern Benguela region (Chris Bartholomae, pers. comm.). This is confirmed by the SST anomalies presented in Figure 19 in the next section. It was thus expected that stronger than usual southerly winds and resultant offshore transport would be found during this period. Similar persistent anomalies could not be identified for the southern Benguela region.

In general, not many prolonged and intense anomalies could be identified from the data used here. This can probably be attributed partially to that fact that the data

series is relatively short, combined with the fact that the data is of a rather coarse spatial resolution.

Date	15	18	23	26	31	33	Date	15	18	23	26	31	33
	°S	°S	°S	°S	°S	°S		°S	°S	°S	°S	°S	°S
07/92						-	03/96			+			
09/92				+	+		05/96	+					
10/92				-	-		08/96	+					-
05/93						-	11/96			-			
07/93				-	-		02/97			+			
10/93				+			03/97						-
02/94						+	07/97	-					
03/94			-	-			08/97		-			+	
06/94	+	+					09/97			-	-		
07/94					+		10/97				-		
08/94						+	11/97				-		
07/95				+			01/98		+		+		
08/95	+	+				-	11/98	+			+		
10/95			-	-			06/99			-			
11/95		-					08/99					-	
12/95				-		+	12/99				-		
01/96					+		10/00	-					

**Table:** Summary of identified anomalies in the alongshore wind stress at the six selected sites.

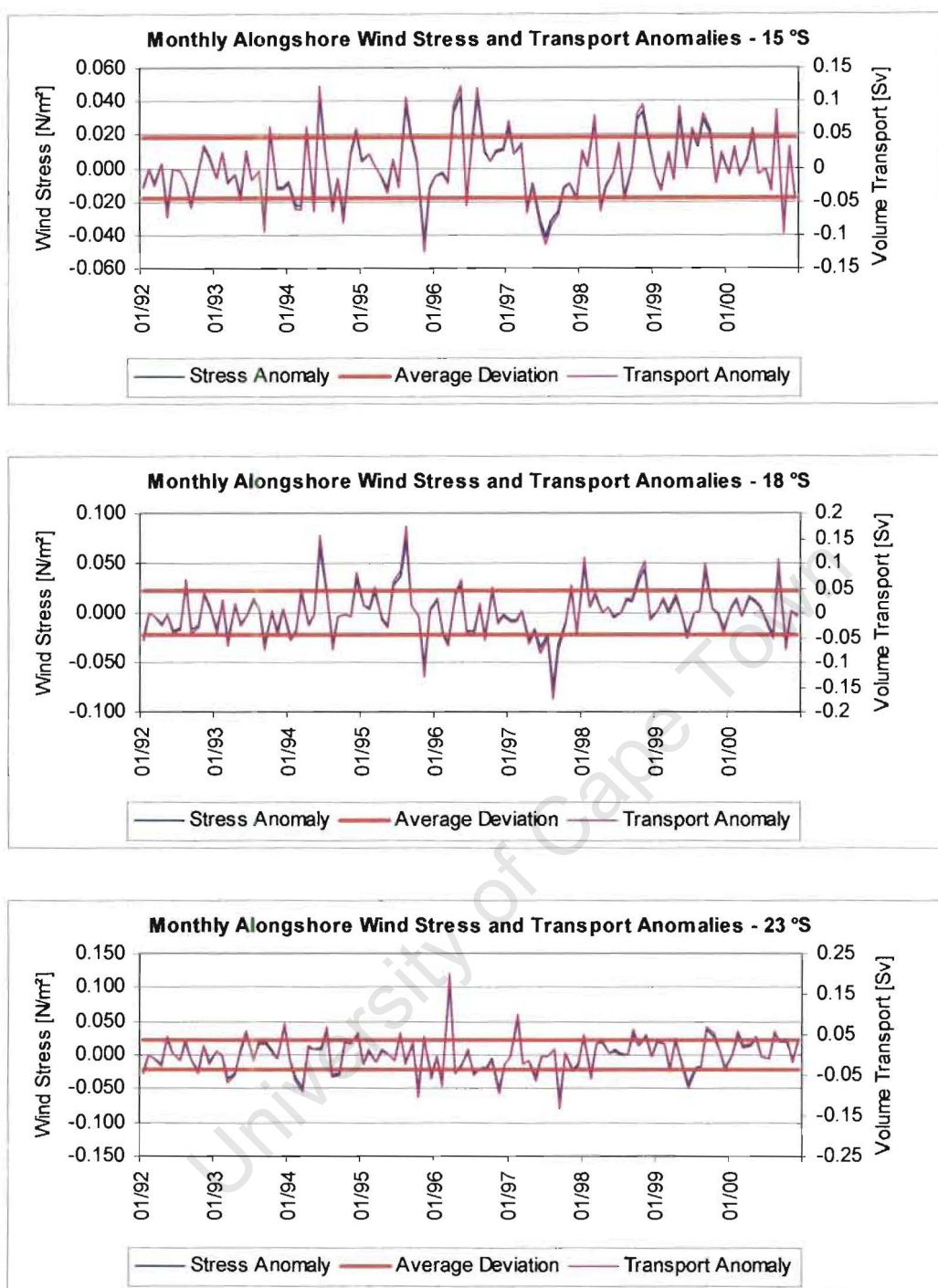


**Figure 17:** Anomalies of the Southerly Wind Stress and Total Volume Transport at Selected Sites with the average of the deviations from the mean



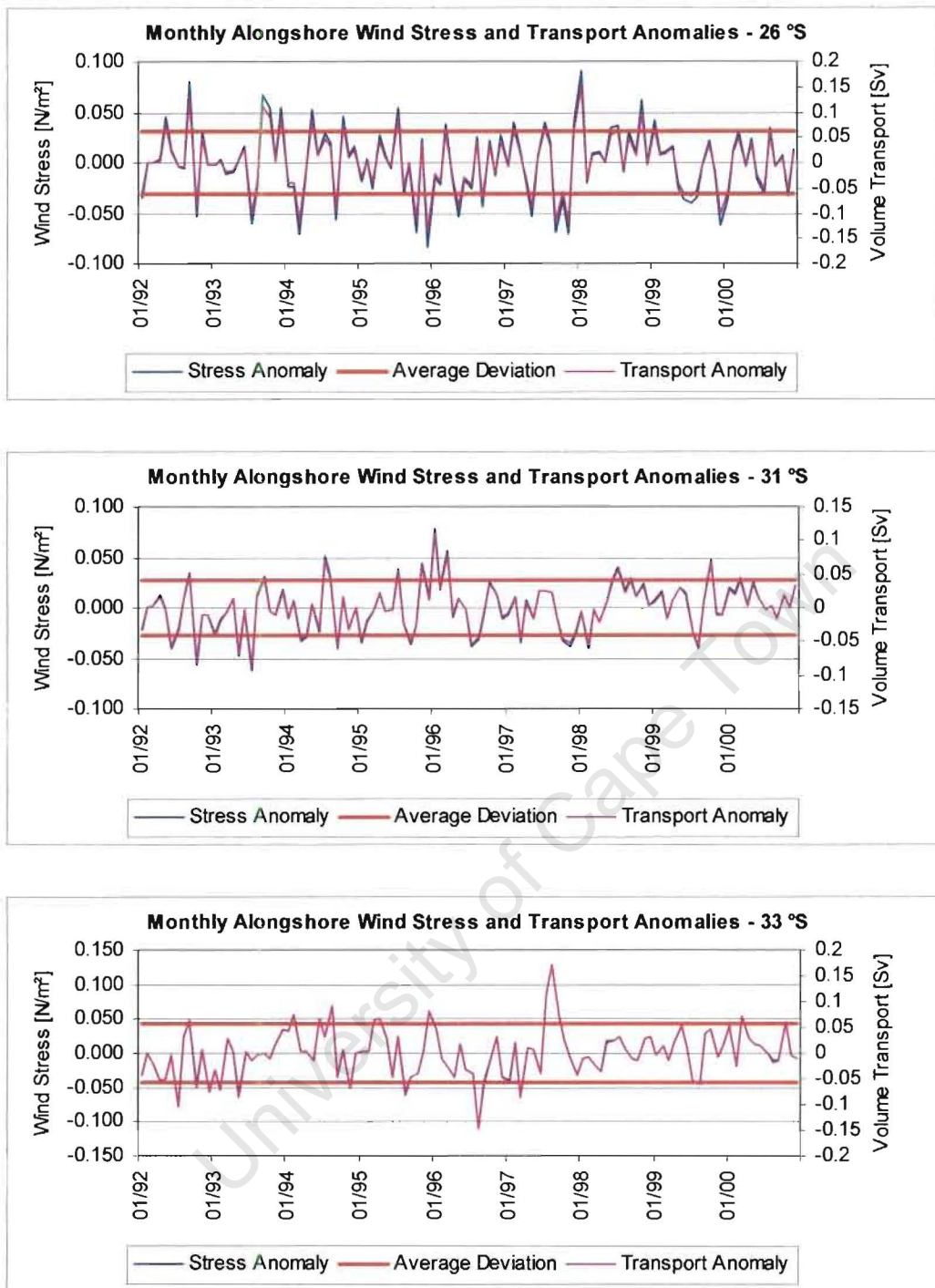


**Figure 17 (contd.):** Anomalies of the Southerly Wind Stress and Total Volume Transport at Selected Sites with the average of the deviations from the mean

It is difficult to compare the pattern of variability in the Ekman transport as little is published on it covering the same period. However, the estimates derived here for the Ekman transport (Figure 18) compared well with that of Johnson and Noli-Perard (1998) and Johnson and Nelson (1999) for Lüderitz Cape Columbine respectively,

considering that this study used a coastline length of 111 km and not 30 km as in those studies. This is despite the fact that in both the cited cases, measurements from coastal weather stations (single location) were used for analysis whereas analysis here are based on scatterometer measurements made by satellite ( $1^\circ \times 1^\circ$ ).

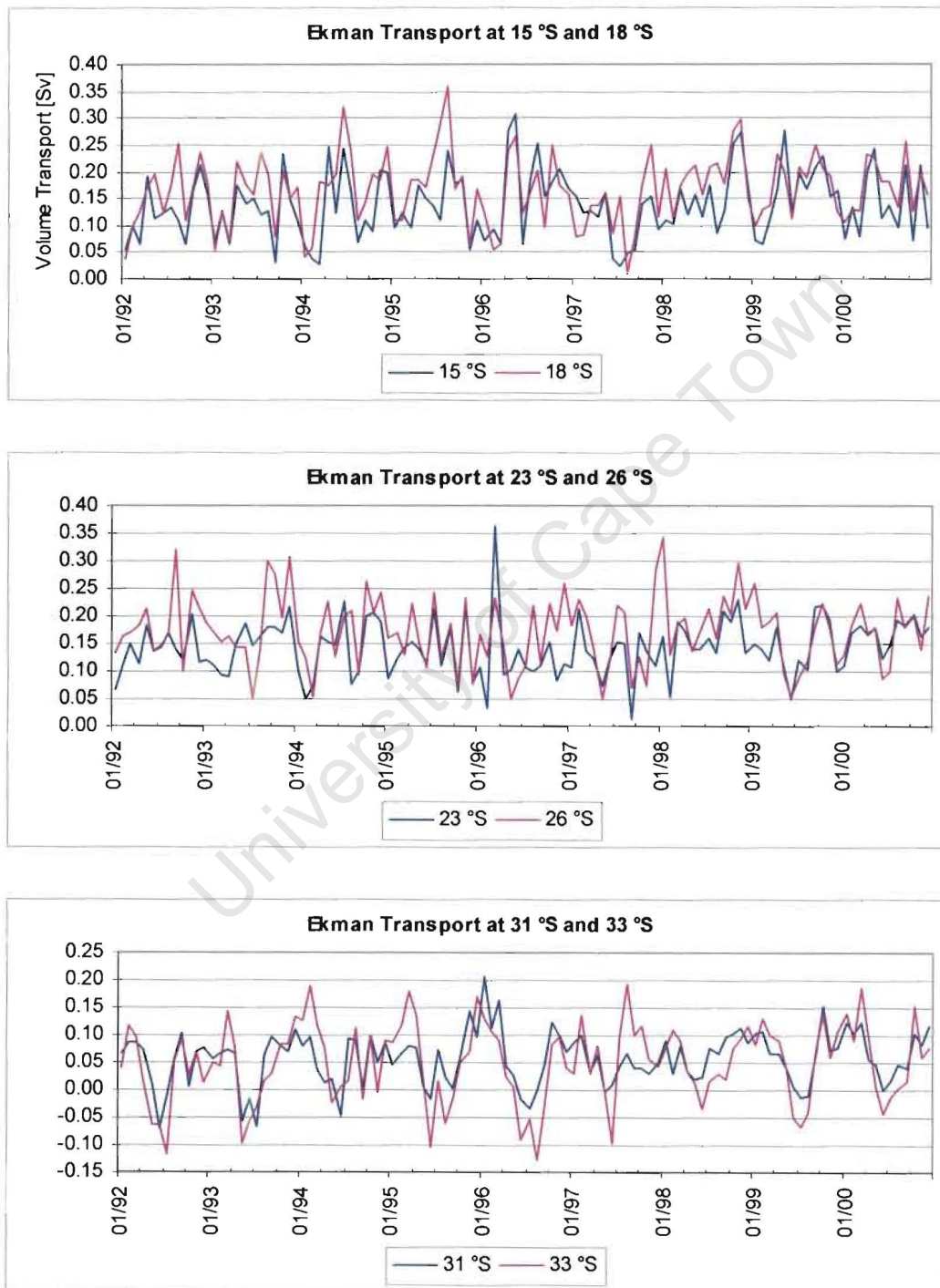


**Figure 18:** Total Volume Transport per  $1^\circ$  Block

## 4.2.2 SEA SURFACE TEMPERATURE

### 4.2.2.1 SEA SURFACE TEMPERATURE ANOMALIES

Figure 19 is a plot of the SST anomalies at the coast during the study period. These were calculated from the three extracted pixels next to the coastline of which the area average was calculated, and represents the deviation from the mean SST of each month for each area (see methods section). The SST anomalies at the selected sites discussed before (see methods section) are plotted in Figure 20.

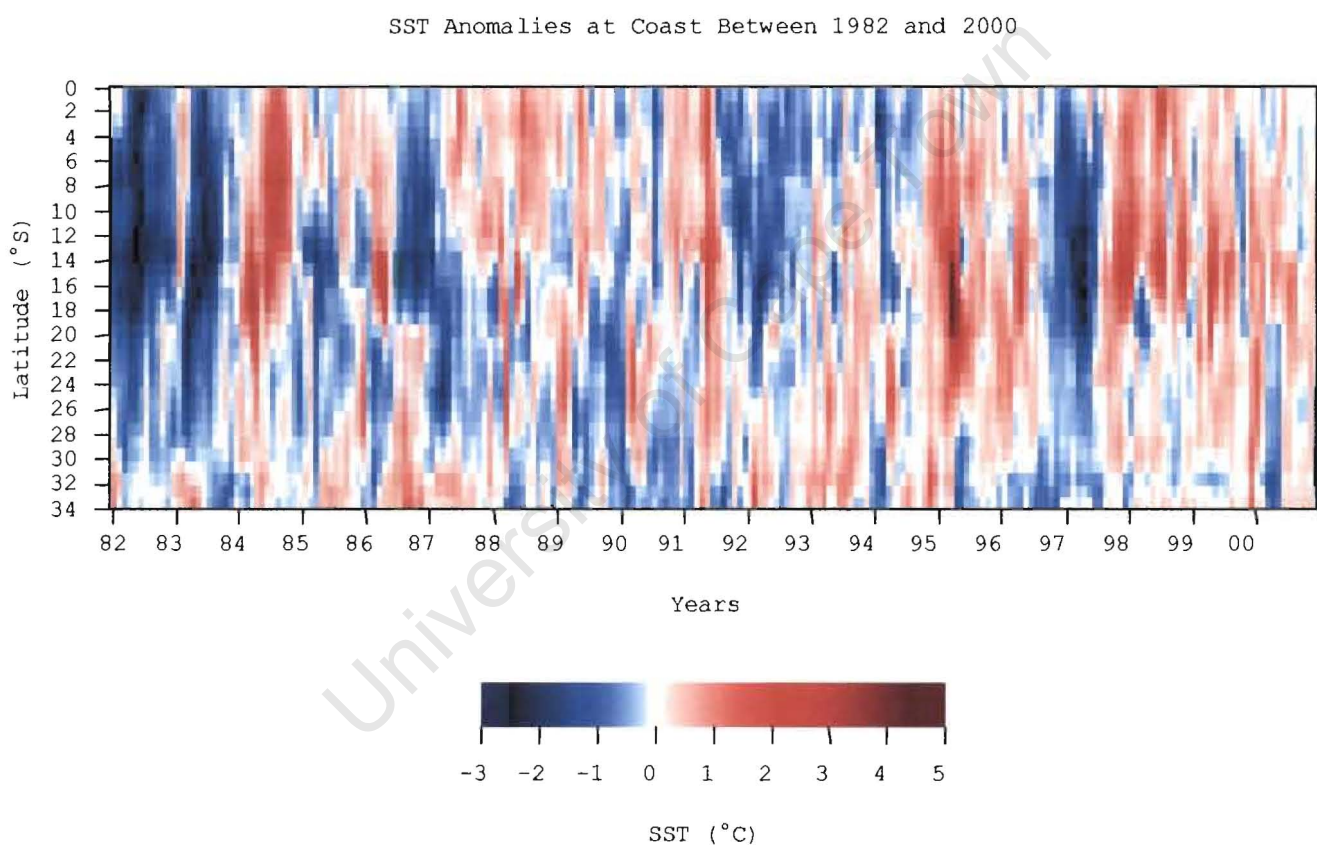


**Figure 19:** SST Anomalies at the Coast (1982 – 2000)

In the previous section it was evident that the Benguela system has a recognizable seasonal SST pattern. Deviations from this general mean seasonal pattern from year to year serve to constitute particular inter-annual patterns of the SST and the SST variability. Over the study period, a great amount of variability in the monthly SST is



observed. Although SST variability in the Benguela is normal, there are periods during which this variability appears to be more intense, leading to anomalous conditions. Anomalies can either be positive (warmer than the long-term mean) or negative (cooler than the long-term mean).

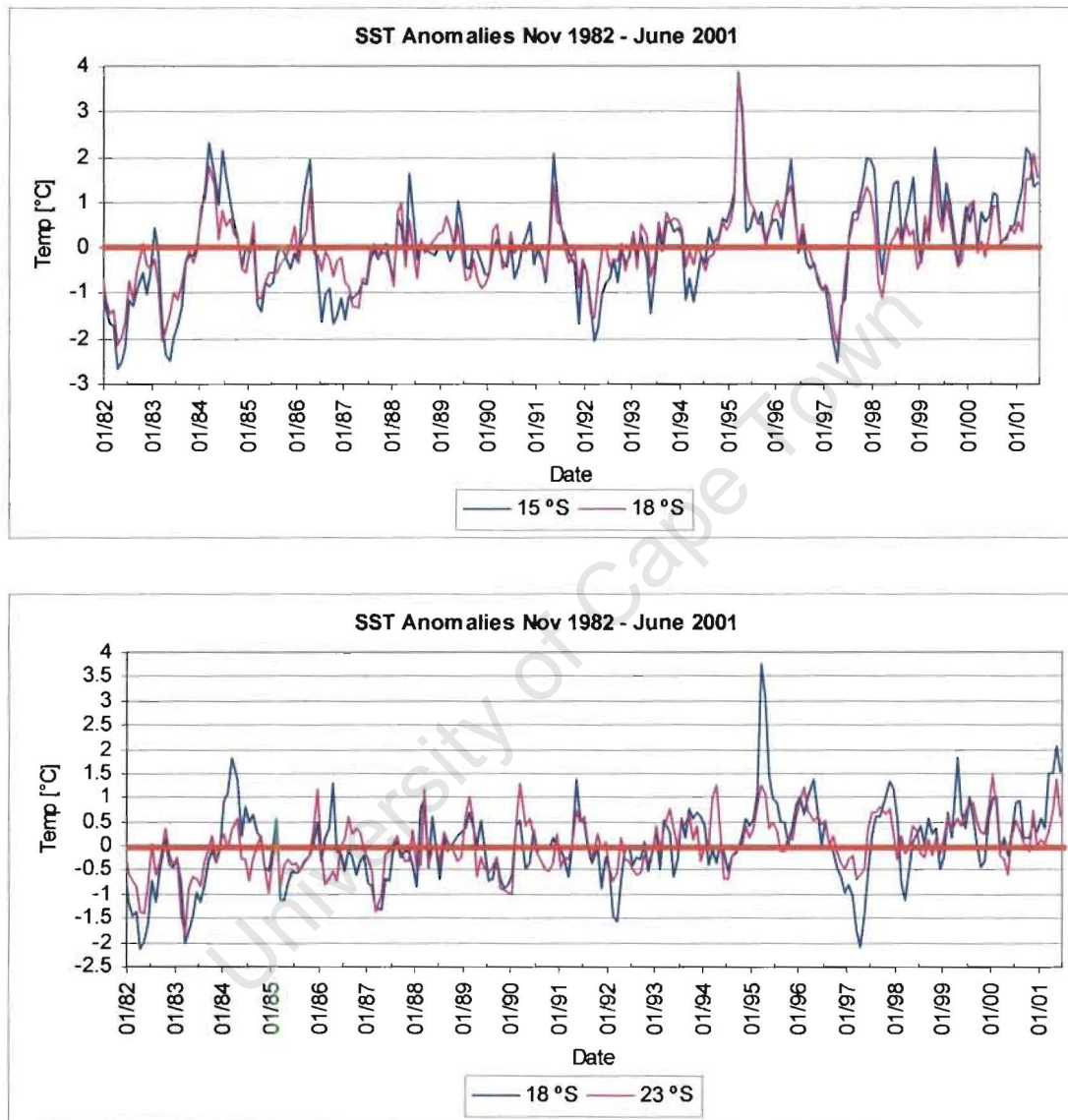


**Figure 20:** SST Anomalies at the Coast for Selected Sites (1982 – 2000)

To avoid classifying shorter, less intense variations in the SST as an anomaly, there is a need to provide some definition as to what constitute a significant SST anomaly. For the purpose of this thesis it has been defined as any deviation, in the SST, of which the absolute value is larger than 1 °C.



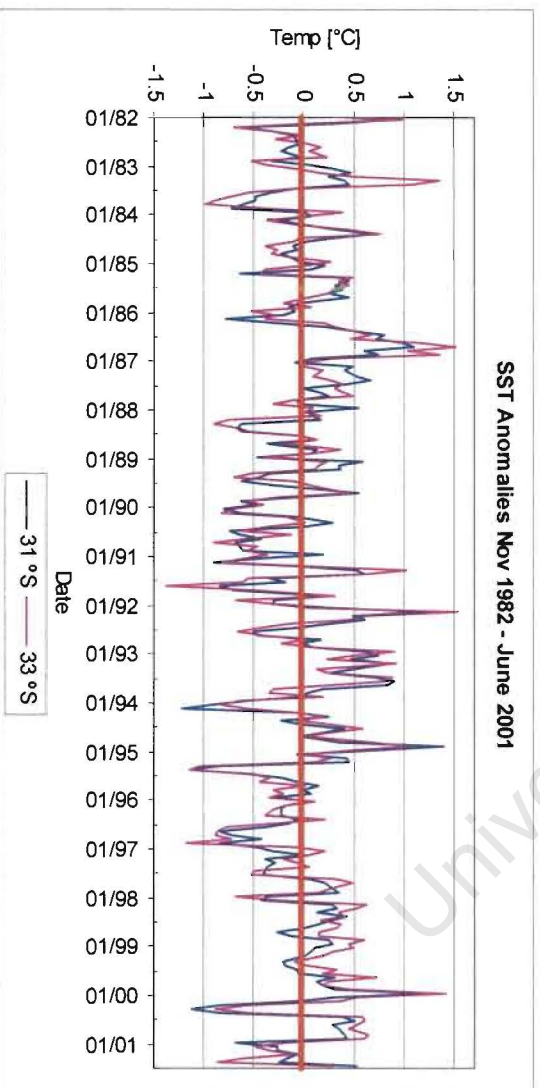
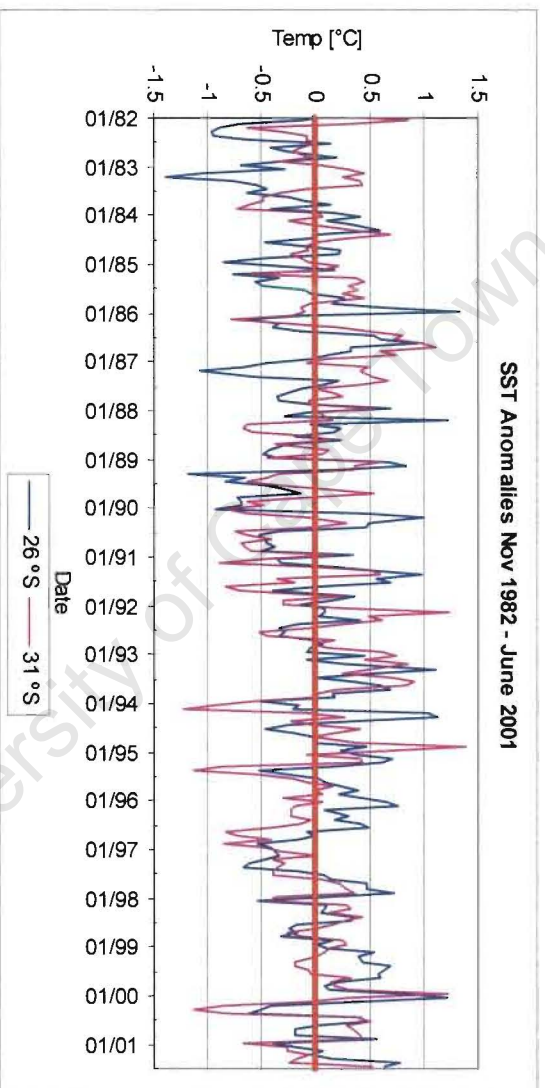
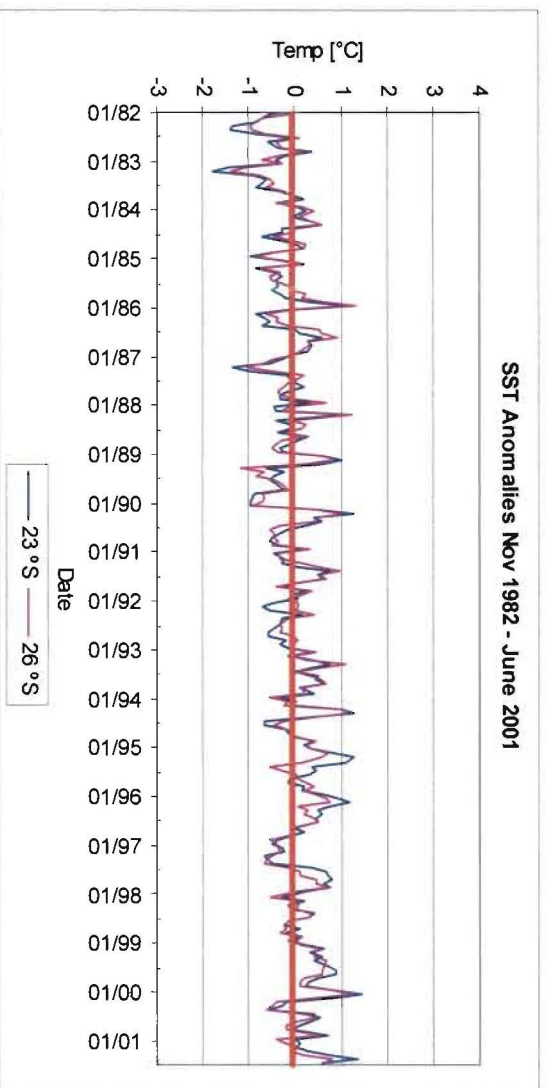


**Figure 20 (contd.):** SST Anomalies at the Coast for Selected Sites (1982 – 2000)

Based on the analysis of the plots in Figures 19 and 20, the following could be derived:

- There are definite differences between the northern and southern parts of the system in terms of the occurrence, intensity and frequency of anomalous events.
- Anomalous event in the northern Benguela (off central and northern Namibia and off southern Angola) appears to “enter” the system from the north, while rarely stretching its influence beyond the Lüderitz area off southern Namibia.

From Figure 19 the following were identified as years during which anomalous events occurred in the system (table below).

	Northern Benguela	Southern Benguela
Cool Periods	1982/3; 1986/7; 1992; 1997	1984; 1989-91; 1996/7; 2000
Warm Periods	1984; 1989-91; 1995; 1998-2000	1983; 1986/7; 1992/3; 1994/5; 1998-2000

The intensities and extent of these anomalous events are varying and they can thus not all be placed in the same category. Strong positive anomalies are observed in the northern part of the system during 1984, beginning 1986 and 1995. Between 1998 and 2000, SST's remained rather high with positive anomalies observed for most of the time. The strongest negative anomalies observed here are during 1982/3, 1987, beginning 1992 and 1997. In the south, the SST anomalies are generally less intense and less pronounced. However, the periods identified in the table above can be taken as being anomalous, even if it does not show similar intensities as in the north.

From the SST anomaly plots of each selected site (Figure 20), the following periods were identified as being anomalous (table below).

	Cool Anomalies	Warm Anomalies
Southern Angola	1982/3; 1986/7; 1992; 1997	1984; 1986; 1991; 1995; 1996; 1998-2000
Northern Namibia	1982/3; 1986/7; 1992; 1997	1984; 1986; 1991; 1995; 1996; 1998-2000
Central Namibia	1982/3; 1987; 1992; 1997	1984; 1986; 1995; 1996; 1998-2000
Southern Namibia	1982/3	1986; 1987; 1999
Northwest South Africa	1991; 1994; 1995; 1997; 2000	1986; 1992; 1995; 1999
Southern South Africa	1991; 1995; end 1996	1983; 1986; 1992; 1999

#### 4.2.2.2 SEA SURFACE TEMPERATURE UPWELLING INDEX (SST UI)

The SST UI (Figure 21) derived using the described method, did not quite yield the expected results. This is probably due to the coarse scale of the original data used in the analysis and the dependence of the index on offshore conditions. Furthermore, this could also be a result, at least to some extent, of fact that three adjacent pixels were combined at the coast for the analysis.

However, it did reveal a number of other features. These being:

- The area north of 16 °S experienced consistently higher SST's at the coast.
- South of 16 °S the SST's at the coast were consistently cooler than offshore.
- Despite the consistently warmer SST's at the coast north of 16 °S, there were periods during which SST's were lower than SST's offshore. This was the

case in 1982, 1983, 1985, 1986, 1990, 1995 and 1996. Since the focus of this study is mainly on the Benguela region as defined earlier, these findings will not be elaborated upon much in further discussions.

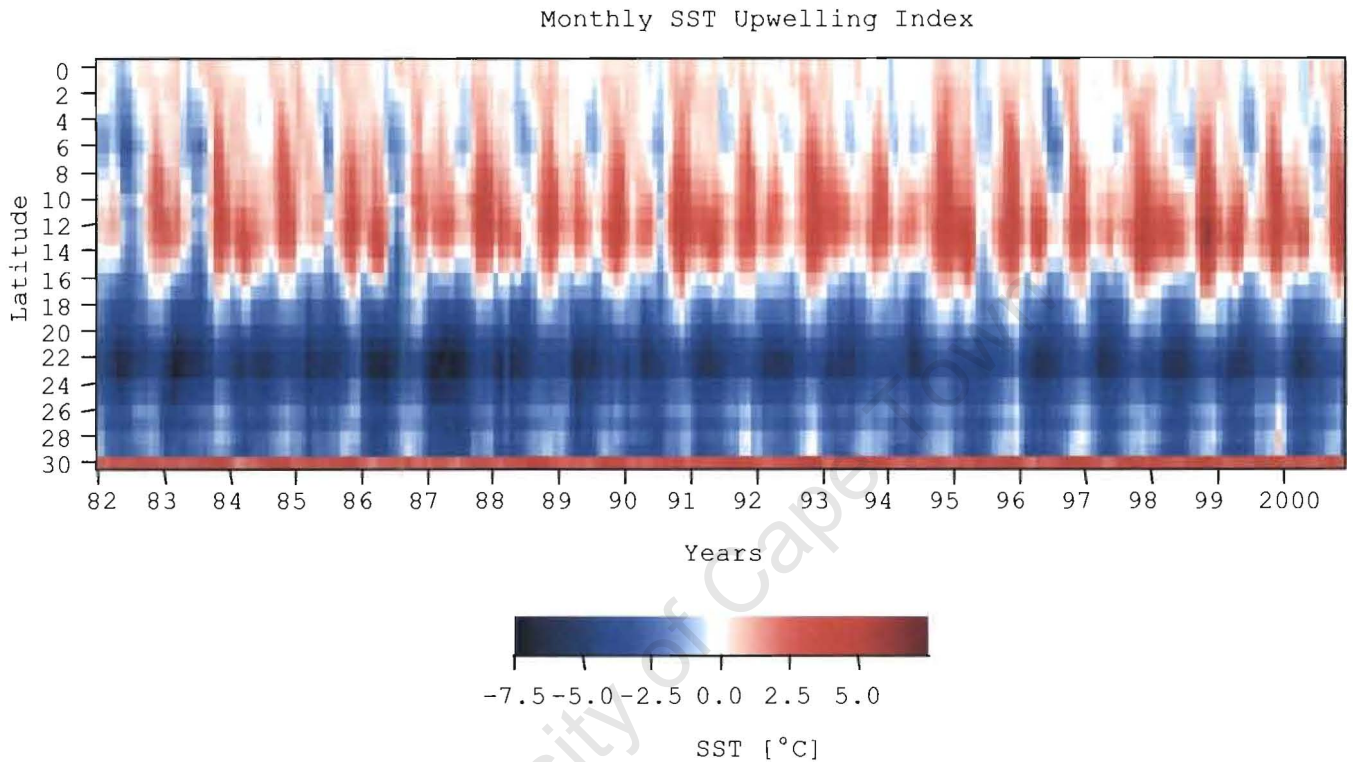


**Figure 21:** SST Upwelling Index (1982 – 2000)

Although warm anomalies in the Benguela upwelling region and elsewhere are relatively well documented, virtually nothing exists on cool anomalies experienced. It is thus possible to compare results from this study with that of others on those warm anomalies identified, but virtually impossible to do the same for the cool anomalies identified. A number of warm anomalies have been identified in this study from the data at hand. However, from the literature, only a few are considered to be of great significance. According to Shannon *et al* (1986), Gamelsrød *et al* (1998) and Binet *et al* (2001), strong Benguela Niño's (warm events) were experienced during 1984 and 1995. Binet *et al* (2001) included 1998 to be a minor Benguela Niño's. Their

analysis included only the years from 1983 up to 1999. Analysis from the study presented here included data of 2000 and up to June 2001. Results suggested that although 1998 was anomalously warm, it does not seem to be an isolated (in time) event. It rather looks like it being part of a prolonged period of warming which lasted up to 2000/1. It is however difficult in the context of this study to describe this warm anomaly as a Benguela Niño as analysis did not include any data on the sub-surface conditions in the region. In his description of a Benguela Niño, Shannon *et al* (1986) discussed the importance of warm water intrusions into the system from the north and the consequent changes in the density structure of the water column. A topic which is not covered by the scope of this thesis.

## 5 SUMMARY OF RESULTS

In this chapter an attempt is made to point out the main features of the SST and upwelling favorable wind conditions over the Benguela upwelling current system as discussed in the previous chapter.

### 5.1 SEASONAL VARIABILITY

#### 5.1.1 WIND FIELDS

- ✓ Upwelling favorable conditions prevail along most of the coast south of 16 °S throughout the year.
- ✓ Some seasonal and latitudinal variations are however observed.
- ✓ A wedge-shape feature, extending offshore and in a northwesterly direction, of strong southerly winds is present throughout most of the year. It appears to intensify during autumn and winter.
- ✓ The area around Lüderitz (~ 25 °S – 27 °S) is experiencing strong upwelling favorable conditions for most of the year with only a slight minimum experienced for a short period during winter. This makes it the most prominent cell of potential upwelling along the coast.
- ✓ In the north (~ 18 °S) near Cape Frio, a secondary cell of potential upwelling can be observed with maxima in April/May, July and October/November.
- ✓ Along the central Namibian coast, between Cape Frio and Lüderitz, upwelling favorable winds also appear to be present throughout the year. However, wind speeds are generally lower.

- ✓ In the south (30 °S – 34 °S), upwelling favorable conditions (strongest southerly winds of speeds between 2.5 m.s<sup>-1</sup> - 6 m.s<sup>-1</sup>) are limited to spring and summer mainly.
- ✓ Near Cape Columbine and the Cape Peninsula in the south (~ 32 °S) upwelling favorable condition (southerly winds) are generally less intense than the potential upwelling cells further north in the system. Between May and July upwelling favorable conditions are completely absent.
- ✓ In general upwelling favorable conditions are more or less perennial between 15 °S and 29 °S.

#### **5.1.2 EKMAN UPWELLING INDEX (EUI)**

- ✓ The largest offshore transport of coastal waters appears to be in the vicinities of Lüderitz and Cape Frio.
- ✓ At Lüderitz high values occur throughout the year with a minimum in winter.
- ✓ At Cape Frio maxima occur during April/May, July and October/November.
- ✓ Along central Namibia (23 °S) seasonality is less pronounced with slight maxima during March, July and November and minima between December and February.
- ✓ In the south, upwelling is restricted to late spring and summer with little or no upwelling during winter.

#### **5.1.3 SST FIELDS**

- ✓ A clear seasonal cycle is observed in the SST fields over the entire area.
- ✓ Warm period spans between October and April with February –April being the warmest.

- ✓ Cool period spans between May and September with July and August being the coolest.
- ✓ Latitudinal differences in SST's are quite obvious with the north being warmer than the south.
- ✓ In the central areas of the study area (mostly along Namibia) SST variability is less than at the latitudinal extremities of the region.
- ✓ Five (5) "SST regions" can be identified along the southwest African coast with each a distinct seasonal pattern.
  - North of 13 °S with SST's > 29 °C.
  - A possible semi-permanent thermal frontal zone between 13 °S and 18 °S with SST's ranging between 20 °C and 26 °C.
  - A moderate zone between 18 °S and 22 °S with SST's ranging between 15 °C and 21 °C through the year.
  - A cooler, less variable zone between 20 °S and 27 °S with SST's between <15 °C and 20 °C.
  - A fifth zone south of 27 °S with mean SST's around 19/20 °C.
- ✓ Lüderitz and surroundings seems to be the coolest for most of the year, suggesting almost perennial upwelling in the area.
- ✓ The greatest seasonal differences in SST are observed in the northern and the southern ends of the system.
- ✓ The highest SST's at all sites occur during mid-summer to autumn (January – April) with the lowest SST's during August/September (late-winter/early-spring).



## **5.2 INTER-ANNUAL VARIABILITY**

### **5.2.1 EKMAN UPWELLING INDEX (EUI) AND SOUTHERLY WIND STRESS ANOMALIES**

- ✓ Weaker than usual southerly winds thus seem to have a greater likelihood of occurrence in the northern Benguela region. This likelihood is reduced to some extent in the southern Benguela.
- ✓ In general, the northern Benguela seems to experience greater variability than the southern Benguela.
- ✓ A significant negatively anomaly was experienced in the northern Benguela between October and December 1995.
- ✓ A longer, more persistent negative anomaly was experienced during July and November 1997 in the northern Benguela. It was especially evident between September and November 1997 in the vicinity of Lüderitz (26 °S).
- ✓ Similar persistent anomalies could not be identified for the southern Benguela region.

### **5.2.2 SST FIELDS**

The combined results of the SST anomalies at the coast and the SST anomalies at selected sites can be summarized as follows:

- ✓ In the northern Benguela cool events occurred during 1982/3, 1986/7, 1992 and 1997. The strongest of these being in 1982, 1983, 1987 and 1997.
- ✓ Warm events in this region occurred during 1984, 1989, 1995 and 1998-2000. Of these the strongest occurred in 1984 and 1995.

- ✓ Significant cool anomalies in the southern Benguela appear to have occurred during 1984, 1989-1991, 1996/7 and 2000.
- ✓ Warm events occurred during 1983, 1986/7 1992/3, 1994/5 and 1998-2000.  
The intensities of these events seem to be of similar magnitude.
- ✓ Between 1998 and 2000, the entire study area seems to be moving in a prolonged warm phase.

University of Cape Town

## 6 CONCLUDING REMARKS

Results obtained in this study were generally in good agreement with that of the literature cited in the text. This leads to the conclusion that, although the data used here were of very coarse spatial resolution, it still showed great value in its application for studies on the large-scale temporal and spatial variability.

With regards to the initial objectives of this study, one can argue that the data proved especially useful in describing the seasonal patterning of both the SST and upwelling favorable wind fields. Analysis of the monthly SST data yielded results on the inter-annual variability and anomalous events that are generally comparing well with that of published work. Both the Ekman Upwelling Index and the SST Upwelling Index failed to describe the inter-annual variability in the region successfully and to clearly highlight strong anomalous events. This may on the one hand be a result of the spatial resolution of data used and on the other hand a result of the techniques used here.

Thorough statistical comparisons between the data used here with *in situ* data would probably enhance the reliability of the dataset and improve results. Results could in future be further improved with the use of statistical techniques in both the processing and analysis of the data.

## 7 BIBLIOGRAPHY

1. Abbot, M.R. and B. Barksdale, 1995. Variability in Upwelling Systems as Observed in Satellite Remote Sensing. In *Upwelling in the Ocean: Modern Processes and Ancient Records*. C. P. Summerhayes, K.-C. Emeis, M. V. Angel, R. L. Smith, and B. Zeitzschel (Eds.). John Wiley & Sons Ltd: 221-238.
2. Andrews, W. R. H. and L. Hutchings, 1980. Upwelling in the Southern Benguela Current. *Prog. Oceanogr.* **9**(1), 81pp.
3. ATSR (2000). The ATSR Project. <http://www.atsr.rl.ac.uk/>.
4. Bakun, A. and C. S. Nelson, 1991. The Seasonal Cycle of Wind-Stress Curl in Subtropical Eastern Boundary Current Regions. *J. Phys. Oceanogr.*, **21**, 1815 – 1834.
5. Bang, N. D., 1971. The Southern Benguela Current Region in February, 1966. 2. Bathymetry and Air-Sea Interactions. *Deep Sea Res.*, **18** (2): 209 – 224.
6. Barber, R. T. and R. L. Smith, 1981. Coastal Upwelling Ecosystems. In *Analysis of Marine Ecosystems*. Longhurst, A. R (Ed.). London; Academic Press: 31 – 68.
7. Bentamy, A., Y. Quilfen, F. Gohin, N. Grima, M. Lenaour and J. Servain, 1996. Determination and Validation of Average Wind Fields from ERS-1 Scatterometer Measurements. *The Global Atmosphere and Ocean System*, Vol 4, 1 - 29.
8. Bentamy, A., P. Queffeulou, B. Chapron and Y. Quilfen, 1997. Quality and Characteristics of NSCAT Backscattering Coefficients and Surface Winds. *CEOS Wind and Wave Validation Workshop, ESA, ESTEC, 3-5 June*. Noordwijk, The Netherlands, 145-157.
9. Binet, D., B. Gobert and L. Maloueki, 2001. El Niño-like warm events in the Eastern Atlantic (6°N, 20°S) and fish availability from Congo to Angola (1964 – 1999). *Aquat. Living Resour.*: **14**, 99 – 113.
10. Boyd, A. J., 1987. *The Oceanography of the Namibian Shelf*. PhD. Thesis, University of Cape Town, [xv] + 190 pp + [i].
11. Boyd, A. J., J. Salat and M. Masó, 1987. The Seasonal Intrusion of Relatively Saline Water on the Shelf off Northern and Central Namibia. In: *The Benguela and Comparavle Ecosystems*. A. I. L. Payne, J. A. Gulland and K. H. Brink (Eds.). *S. Afr. J. mar. Sci.*: **5**, 107 – 120.
12. Brundrit, G. B., 1984. Monthly Mean Sea Level Variability Along the West Coast of Southern Africa. *S. Afr. J. mar. Sci.*: **2**, 195 – 203.

13. Brundrit, G. B., 1995. Trends of Southern African Sea Level: Statistical Analysis and Interpretation. *S. Afr. J. mar. Sci.*: **16**, 9 – 17.
14. Cole, J.F.T., 1997. *The Surface Dynamics of the Northern Benguela Upwelling System and its Relationship to Patterns of Clupeoid Production*. PhD Thesis. University of Warwick, Coventry, UK. 208 p.
15. Cole, J. F. T. and J. McGlade, 1998. Temporal and Spatial Patterning of Sea Surface Temperature in the Northern Benguela Upwelling System: Possible Environmental Indicators of Clupeoid Production. In: *Benguela Dynamics*. S. C. Pillar, C. L. Moloney, A. I. L. Payne and F. A. Shillington (Eds.). *S. Afr. J. mar. Sci.*: **19**, 143 – 157.
16. Emery, W. J. and R. E. Thomson, 1998. *Data Analysis Methods in Physical Oceanography*. 1<sup>st</sup> ed. Pergamon, New York, 634 pp.
17. Gammelsrød, T., C. H. Bartholomae, D. C. Boyer, V. L. L. Filipe and M. J. O'Toole, 1998. Intrusion of Warm Surface Water Along the Angolan-Namibian Coast in February – March 1995: The 1995 Benguela Niño. In: *Benguela Dynamics*. S. C. Pillar, C. L. Moloney, A. I. L. Payne and F. A. Shillington (Eds.). *S. Afr. J. mar. Sci.*: **19**, 41 – 56.
18. Graber, H., N. Ebuchi and R. Vakkayil, 1996. Evaluation of ERS-1 scatterometer winds with wind and wave ocean buoy observations. *Jet Propulsion Laboratory (JPL), National Aeronautic and Space Administration (NASA), National Space Agency of Japan (NASDA)*, 78 pp.
19. Hallerman and Rosenstein, 1983. Normal Monthly Windstress over the World Ocean with Error Estimates. *J. Phys. Oceanogr.*, **13**, 1093 - 1104.
20. Hardman-Mountford, N. J., 2000. *Environmental variability in the Gulf of Guinea Large Marine Ecosystem: Physical features, forcing and fisheries*. PhD. Thesis, University of Warwick, 312 pp.
21. Hart, T. J. and R. I. Currie, 1960. The Benguela Current. "*Discovery*" Rep. 31: 123 – 297.
22. Hill, A. E., B. M. Hickey, F. A. Shillington, P. T. Strub, K. H. Brink, E. D. Barton and A. C. Thomas, 1998. Eastern Ocean Boundaries. *The Sea*: **11**, A. R. Robinson and K. H. Brink (Eds.), John Wiley & Sons, New York, pp. 29 – 67.
23. Hunter, I. T., 1987. The Weather of the Ahulhas and Cape South Coast. *CSIR Research Report*, 634: 148 pp.
24. Hutchings, L. and J. Taunton-Clark, 1990. The Monitoring of Gradual Change in Areas of High Mesoscale Variability. *S. Afr. J. Sci.*, **86**, 9 – 37.

25. Johnson, A. S. and G. Nelson, 1999. Ekman Estimates of Upwelling at Cape Columbine Based on Measurements of Longshore Wind from a 35-Year Time-Series. *S. Afr. J. mar. Sci.*: **21**, 433 – 436.
26. Johnson, A. S. and K. Noli-Pearl, 1998. Ekman Estimates of Upwelling Derived from Winds Measured at Lüderitz. Poster: *International Symposium on Environmental Variability in the Benguela Current, 30 March – 01 April 1998*. Swakopmund, Namibia.
27. Jury, M. R., 1988. Case Studies of the Response and Spatial Distribution of Wind-Driven Upwelling off the Coast of Africa: 29 – 34 ° South. *Cont. Shelf Res.*, **8**(11), 1257 – 1271.
28. Jury, M. R., C. I. MacArthur and G. B. Brundrit, 1990. Pulsing of the Benguela Region: Large-Scale Atmospheric Controls. *S. Afr. J. mar. Sci.*: **9**, 27 – 41.
29. Kamstra, F., 1985. Environmental Features of the Southern Benguela with Special Reference to the Wind Stress. *South African Ocean Color Experiment*. L. V. Shannon (Ed.), Cape Town, Sea Fisheries Research Institute: 13 – 27.
30. Kidwell, K. B., 1991. *NOAA Polar Orbiter Data Users Guide*. NOAA, Satellite Data Services Division, World Weather Building, Washington, DC.
31. Lillesand, T.M. and R.W. Kiefer (1994). *Remote Sensing and Image Interpretation*. John Wiley and Sons, New York, 721 pp.
32. Lutjeharms, J. R. E. and J. M. Meeuwis, 1987. The Extent and Variability of South-East Atlantic Upwelling. In: *The Benguela and Comparable Ecosystems*. A. I. L. Payne, J. A. Gulland and K. H. Brink (Eds.). *S. Afr. J. mar. Sci.* **5**, 51 – 62.
33. Lutjeharms, J. R. E. and P. L. Stockton, 1987. Kinematics of the Upwelling Front off Southern Africa. In: *The Benguela and Comparable Ecosystems*. A. I. L. Payne, J. A. Gulland and K. H. Brink (Eds.). *S. Afr. J. mar. Sci.* **5**, 35 – 49.
34. Lutjeharms, J. R. E., F. A. Shillington and C. M. Duncombe Rae, 1991. Observations of Extreme Upwelling Filaments in the Southeast Atlantic Ocean. *Science (N.Y.)*, **253** (5021). 774 – 776.
35. Mann, K. H. and J. R. N. Lazier, 1991. *Dynamics of Marine Ecosystems*. Blackwell, Boston, 466 pp.
36. Maul, G. A., 1985. *Introduction to Satellite Oceanography*. Kluwer Academic Publishers, Dordrecht, 606 pp.

37. Meeuwis, J. M. and J. R. E. Lutjeharms, 1990. Surface Thermal Characteristics of the Angola-Benguela Front. *S. Afr. J. Mar. Sci.*, **9**, 261 – 279.
38. Moroshkin, K. V., V. A. Bubnov and R. P. Bulatov, 1970. Water Circulation in the Eastern South Atlantic Ocean. *Oceanology* **10** (1): 27 – 34.
39. Nelson, G. and L. Hutchings, 1983. The Benguela Upwelling Area. *Prog. Oceanog.*: **12**, 333 – 356.
40. Nelson, G. and N. Walker, 1984. Comparison of Summer Winds on the West Coast of South Africa Between 1979 and 1983 and the Response of Coastal Upwelling. *S. Afr. J. Sci.*: **80**, 90 – 93.
41. Nelson, G., 1989. Poleward Motion in the Benguela Area. In: *Poleward Flows along Eastern Ocean Boundaries*. S. J. Neshyba, C. N. K. Mooers, R. L. Smith and R. T. Barber (Eds.). Springer, New York, 110 – 130.
42. Nykjær, L. and L. Van Camp, 1994. Seasonal and Interannual Variability of Coastal Upwelling along Northwest Africa and Portugal from 1981 to 1991. *J. Geophys. Res.*: **99**, 14,197 – 14,207.
43. Parrish, R.H., A. Bakun, D.M. Husby and C.S. Nelson (1983). Comparative climatology of selected environmental processes in relation to eastern boundary current pelagic fish reproduction. In: *Proceedings of the Expert Consultation to Examine Changes in Abundance and Species Composition of Neritic Fish Resources, San José, Costa Rica*. G. D. Sharp and J. Csirke (Eds.). FAO Fisheries Reports **293**(3): 731-777.
44. Pond, S. and G. L. Pickard, 1983. *Introductory Dynamical Oceanography*. 2<sup>nd</sup> ed. Pergamon, New York, 329 pp.
45. Preston-Whyte, R. A. and P. D. Tyson, 1988. *The Atmosphere and Weather of Southern Africa*. Oxford University Press, Cape Town, 475 pp.
46. Reynolds, R. W., 1988: A real-time global sea surface temperature analysis. *J. Climate*, **1**, 75-86.
47. Reynolds, R. W. and D. C. Marsico, 1993: An improved real-time global sea surface temperature analysis. *J. Climate*, **6**, 114-119.
48. Reynolds, R. W. and T. M. Smith, 1994: Improved Global Sea Surface Temperature Analyses. *J. Climate*, **7**, 929 - 948.
49. Reason, C. J. C. and M. R. Jury, 1990. On the Generation and Propagation of the Southern African Coastal Low. *Q. J. R. Meteorol. Soc.*, **116**, 1133 – 1151.
50. Shannon, L. V., 1985. The Benguela Ecosystem Part I. Evolution of the Benguela Physical Features and Processes. *Oceanogr. Mar. Biol. Ann. Rev.*: **23**, 105 – 182.

51. Shannon, L. V., A. J. Boyd, G. B. Brundrit and J. Taunton-Clark, 1986. On the Existence of an El Niño-type Phenomenon in the Benguela System. *J. Mar. Res.*: **44**, 495 – 520.
52. Shannon, L. V., J. J. Agenbag and M. E. L. Buys, 1987. Large- and Mesoscale Features of the Angola-Benguela Front. In: *The Benguela and Comparavle Ecosystems*. A. I. L. Payne, J. A. Gulland and K. H. Brink (Eds.). *S. Afr. J. mar. Sci.* **5**, 11 – 34.
53. Shannon, L. V. and G. Nelson, 1996. The Benguela: Large Scale Features and Processes and System Variability. In: *The South Atlantic: Past and Present Circulation*. G. Wefer, W. H. Berger, G. Seidler and D. J. Webb (Eds.). Springer-Verlag, Berlin, Heidelberg, 163 – 210.
54. Shillington, F. A., W. T. Peterson, L. Hutchings, T. A. Probyn, H. N. Waldron and J. J. Agenbag, 1990. A Cool Upwelling Filament off Namibia, Southwest Afriac: Preliminary Measurements of Physical and Biological Features. *Deep-Sea Research*, **37** (11), 1753 – 1772.
55. Shillington F. A., 1998. The Benguela Upwelling System off Southwest Africa. *The Sea*: **11**, A. R. Robinson and K. H. Brink (Eds.), John Wiley & Sons, New York, pp. 583 – 604.
56. Smith, R. L., 1995. The Physical Processes of Coastal Ocean Upwelling Systems. In: *Report of the Dahlem Workshop on Upwelling in the Ocean: Modern Processes and Ancient Records, Berlin 1994, September 25-30. Environmental Sciences Research Report Vol. ES 18*. C. P. Summerhayes, K.-C. Emeis, M. V. Angel, R. L. Smith, and B. Zeitzschel (Eds.). John Wiley & Sons, Chichester, West Sussex, UK. pp. 39-64.
57. Van Camp, L., L. Nykjær, E. Mittelstaedt and P. Schlittenhardt, 1991. Upwelling and Boundary Circulation off Northwest Africa as Depicted by Infrared and Visible Satellite Observations. *Prog. Oceanogr.*, **26**, 357 – 402.
58. Van Foreest, D., F. A. Shillington and R. Legeckis, 1984. Large Scale, Stationary, Forntal Features in the Benguela Current System. *Cont. Shelf Res.*, **3** (4), 465 – 474.
59. Walker, N., J. Taunton-Clark and J. Pugh, 1984. Sea Temperatures off the South African West Coast as Indicators of Benguela Warm Events. *S. Afr. J. Sci.*: **80**, 72 – 76.
60. Walker, N.D., 1987. Interannual Sea Surface Temperature Variability and Associated Atmospheric Forcing within the Benguela System. In: *The Benguela and Comparavle Ecosystems*. A. I. L. Payne, J. A. Gulland and K. H. Brink (Eds.). *S. Afr. J. mar. Sci.* **5**, 121 – 132.